

Spacing gain and absorption in a simple \mathcal{PT} -symmetric model: spectral singularities and ladders of eigenvalues and resonances

D. I. Borisov^{1,2,3}

¹Institute of Mathematics, Ufa Federal Research Center,
Russian Academy of Sciences, Ufa, Russia, 450008

²Bashkir State Pedagogical University named after M.Akhmulla, Ufa, Russia, 450000

³University of Hradec Králové, Hradec Králové 50003, Czech Republic

D. A. Zezyulin⁴

⁴ITMO University, St. Petersburg 197101, Russia

August 20, 2019

Abstract

We consider a parity-time (\mathcal{PT} -) symmetric waveguide consisting of a localized gain and loss elements separated by a variable distance. The situation is modelled by a Schrödinger operator with localized complex \mathcal{PT} -symmetric potential. Properties of the latter Hamiltonian are considered subject to the change of the gain-to-loss distance. Resonances, spectral singularities and eigenvalues are analyzed in detail and discussed in the context of the associated laser-absorber modes and \mathcal{PT} -symmetry breaking phase transition. Increasing gain-to-loss distance creates new resonances and spectral singularities which do not exist in the waveguide with adjacent gain and loss. In the limit of large gain-to-loss distance, the waveguide features a ladder of resonances which can be transformed to a ladder of complex eigenvalues by means of the change of the gain-and-loss amplitude.

1 Introduction

Waves interacting with localized parity-time (\mathcal{PT} -) symmetric potentials feature a variety of novel and interesting phenomena, such as scattering resonances at real energies [1], coherent perfect absorption and lasing operation [2], loss-induced lasing [3], invisibility effects [4] and others. The simplest realization of a \mathcal{PT} -symmetric system couples a pair of geometrically identical elements with energy gain and absorption [5]. This idea was, in particular, elaborated in the context of electromagnetic waveguides [1, 6], coupled optical structures [7, 8], and in many other physical environments, see reviews [9, 10, 11, 12, 13]. Behavior of many bicentric \mathcal{PT} -symmetric structures can be modelled by effective Schrödinger-like Hamiltonians, which are usually non-self-adjoint (with respect to the standard inner product). In the present paper, we consider a one-dimensional Hamiltonian with a generalized \mathcal{PT} -symmetric step potential consisting of a pair of identical gain and loss elements separated by a variable distance. We aim to study the spectral properties of this operator as the distance varies. In our study, we mostly focus on two aspects. The first direction concerns the spectral properties of our operator as the distance between gain and loss elements is large. We demonstrate that in this regime our simple bicentric \mathcal{PT} -symmetric Hamiltonian features a ladder of resonances resembling the well-known Wannier-Stark ladder for periodic Hamiltonians with an additional potential gradient [14]. Upon the change of the gain-and-loss amplitude the ladder of resonances can be transformed to a ladder of complex-conjugate pairs of eigenvalues and vice versa. This

behavior has no counterpart in the self-adjoint case. Transformation from a resonance to an eigenvalue corresponds to a zero-width resonance, i.e. to a spectral singularity in the continuous spectrum [1]. A detailed study of spectral singularities and associated \mathcal{PT} -phase transition under the change of the gain-to-loss distance is the second objective of our work.

To the best of the authors' knowledge, \mathcal{PT} -symmetric problems with gain and losses separated by a large distance, were not studied before. At the same time, this regime was studied in details for self-adjoint Schrödinger operators with two (or several) potential wells separated by a large distance. Not trying to cite all papers in this direction, we mention several classical works [15, 16, 17, 18, 19, 20] and a series of very recent ones [21, 22, 23, 24]. The classical works addressed the case of several wells, while in the recent works the wells were replaced by localized abstract operators, including such examples as second order operators with compactly supported coefficients, localized geometric perturbation, delta-potentials on compact manifolds, etc. The main results concerned the behavior as the distances between localized wells or operators tends to infinity. In such a regime, the resolvent of the original operators is approximated in the norm resolvent sense by the direct sum of the resolvents for each well or localized operator. The most general results of such kind were obtained in [21, 23]. The eigenvalues and the associated eigenfunctions in such regime also attracted a lot of interest. In the classical works, the leading terms of their asymptotics were obtained. A general scheme allowing to construct complete asymptotic expansions in the most general setting was proposed in [24]. We also mention work [22], in which the localized operators were modeled by change of type of boundary conditions and there were studied resonances emerging from the eigenvalues embedded into the essential spectrum.

As we have mentioned above, in the large distance regime we find a phenomenon similar to Wannier-Stark resonances; let us briefly recall the matter of such resonances. Wannier-Stark resonances or Wannier-Stark ladders is a celebrated topic studied both by physicists and mathematicians, see, for instance, papers [14, 25, 26, 27, 28, 29]. Here the main object the study is a Schrödinger operator with a fixed periodic potential and a linear potential with a small coupling constant like

$$-\frac{d^2}{dx^2} + V_{per}(x) + \varepsilon x \quad \text{on } \mathbb{R}. \quad (1.1)$$

The main phenomenon is that as $\varepsilon \rightarrow 0$, such operator has a growing number of resonances accumulating to some zone in the essential spectrum. Namely, the imaginary parts of these resonances and the distances between two neighbouring resonances tend to zero, that is, there is a ladder of resonances in the vicinity of some part of the essential spectrum. A distinctive feature of this phenomenon is that the mentioned zone in the essential spectrum *contains no spectral singularities* of the considered operator as $\varepsilon = 0$. In fact, the ladder of mentioned resonances can be regarded as emerging from the eigenvalues of the operator $-\frac{d^2}{dx^2} + \varepsilon x$ accumulating on the real axis as $\varepsilon \rightarrow +0$. The main obtained results describe the total number and the asymptotic behavior of these resonances. Wannier-Stark ladders and the associated Bloch oscillations have been addressed theoretically for a \mathcal{PT} -symmetric version of operator (1.1) in [30] and realized experimentally in synthetic \mathcal{PT} -symmetric photonic lattices [31, 32].

In contrast to the conventional, Hermitian operators, in \mathcal{PT} -symmetric systems, scattering resonances have more chances to occur at real energies, i.e. at interior points of the continuous spectrum [1, 33]. A real-energy resonance has zero width and corresponds to a spectral singularity [34, 35, 36, 37], i.e. to a real pole of the resolvent. Additional source of steady interest in spectral singularities originates in the associated regime of laser-antilaser operation [2, 37, 38]: at the spectral singularity the system admits a pair of linearly independent solutions, one of which has a form of a coherent bidirectional outgoing radiation ("laser"), and another solution is a coherently absorbed incident radiation ("antilaser" [39] or coherent perfect absorber (CPA) [40, 41, 42]). Under a small perturbation of the \mathcal{PT} -symmetric operator, the spectral singularity can split either in a pair of resonances or in a complex-conjugate pair of discrete eigenvalues bifurcating from an interior point of the continuous spectrum [43, 44, 45, 46, 47, 48]. The latter situation is related to a peculiar scenario of an exceptional-point-free \mathcal{PT} -symmetry phase transition from purely real to complex spectrum [44, 45, 47], which is distinctively different from the better studied \mathcal{PT} -phase transition through an exceptional point [49, 50]. The detailed study of spectral

singularities and the associated phase transition in the simple \mathcal{PT} -symmetric system with a variable gain-to-loss distance is the second goal of the present paper.

In the present paper we consider a one-dimensional \mathcal{PT} -symmetric Schrödinger operator with a complex potential formed by two localized parts describing losses and gain and separated by some distance. The second parameter in the model is the gain-and-loss amplitude. We study the resonances and the eigenvalues of this model. We derive a compact equation describing the location of the corresponding finite- and zero-width resonances as well as the emergence of localized bound states associated with discrete complex-conjugate eigenvalues. Then we prove a series of qualitative properties of these objects, namely, that there are countably many resonances accumulating at infinity and only finitely many eigenvalues and all of them are symmetric with respect to the imaginary axis. We provide explicit description of the domains in the complex plane, in which the presence of the eigenvalues and resonances is ensured.

The first main result concerns the asymptotic limit of infinitely large distance between the gain and loss. It turns out that in such regime, there exists a ladder of resonances or eigenvalues accumulating in the vicinity of a certain zone of the essential spectrum. This zone is an explicitly found segment starting at zero. We show that as the distance exceeds a certain explicitly given threshold, there are N eigenvalues or resonances in the vicinity of the mentioned segment, where N is also given explicitly in terms of the distance. We also find an asymptotic four-terms approximations for these eigenvalues and resonances with explicitly written terms. These approximations show that the loss-and-gain amplitude determines what kind of objects, eigenvalues or resonances, we deal with, while the distance is responsible for the number of these objects and their distribution. As the distance grows, these eigenvalues or resonances go closer to each other and also tend to the real axis, and this is exactly the same picture as for the Wannier-Stark resonances. At the same time, as we discuss in Section 4, the nature of this ladder is different from Wannier-Stark's case. There are several advantages of our model. The first of them is that such picture is generated not by a linear potential multiplied by a small parameter, but simply by spacing two compactly supported potentials. Thanks to the \mathcal{PT} -symmetry, we can generate not only resonances, but also eigenvalues(!), which is a completely new phenomenon indicating once again how rich the spectra of \mathcal{PT} -symmetric operators are. In comparison to a rather complicated for analysis operator (1.1), our model is much simpler, and this is why we are able to find explicitly the most important characteristics like the total number of zeroes, the threshold for the distance ensuring such phenomenon and several terms in the asymptotic expansions for eigenvalues or resonances.

We also study zero-width resonances of our model. Using a combination of analytical and numerical approaches, we show that the increase of the gain-to-loss distance can drive the \mathcal{PT} -symmetric waveguide through a sequence of self-dual spectral singularities each of which corresponds to the laser-antilaser regime and leads either to the emergence of a new pair of complex-conjugate eigenvalues or to the immersion of the complex-conjugate pair in the continuum. Practical importance of our findings consists in the possibility to use the distance between the gain and loss as a parameter allowing to decrease the \mathcal{PT} -symmetry breaking laser-antilaser threshold: this means that in a waveguide with mutually spaced gain and losses the laser-antilaser regime can be achieved at a smaller gain-and-loss strength than in a waveguide with the adjacent gain and loss elements. The distance between the gain and loss elements enables an additional degree of freedom which allows to achieve a spectral singularity at any real wavenumber given beforehand and also to achieve two spectral singularities simultaneously.

The content of this paper is organized as follows. In Section 2 we introduce the \mathcal{PT} -symmetric model and the basic terminology, and derive the main equation determining the location of resonances and eigenvalues in the complex plane. In Section 3 we prove a series of lemmata describing the properties of complex roots. In Section 4 we apply the proven statements in order to characterize the general picture of the location and behavior of the zeroes in the complex plane and we discuss the ladders of eigenvalues and resonances accumulating to the essential spectrum. Section 5 is devoted to the detailed study of the spectral singularities of \mathcal{PT} -phase transition. Section 6 concludes the paper.

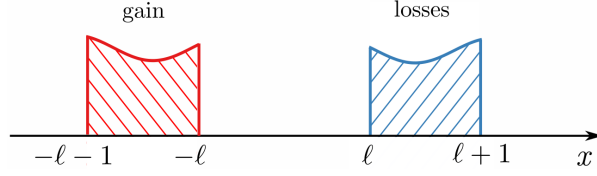


Figure 1: Schematics of a localized potential which consists of a pair of geometrically identical active (gain) and absorptive (losses) elements which are of unitary width and separated by the distance 2ℓ .

2 \mathcal{PT} -symmetric waveguide with spaced gain and loss

2.1 General model and periodicity in the gain-to-loss distance

We consider stationary scattering on a spatially localized \mathcal{PT} -symmetric potential $V(x)$:

$$-\psi_{xx} + V(x)\psi = \lambda\psi, \quad \lambda = k^2, \quad x \in \mathbb{R}, \quad (2.1)$$

where λ is the eigenvalue and k is the complex wavenumber. The complex potential $V(x)$ describes the internal structure of the waveguide. We consider a pair of geometrically identical elements with gain and loss separated by some distance. Since in this work we are primarily interested in the role of the gain-to-loss distance, we assume that the width of each element is scaled to unity. In order to model this situation, we introduce a complex-valued function $W(x)$ compactly supported in the interval $(0, 1)$, and consider a localized complex potential in the form (see figure 1)

$$V(x) = \begin{cases} W(x + \ell + 1) & \text{for } x \in (-\ell - 1, -\ell), \\ \overline{W}(-x + \ell + 1) & \text{for } x \in (\ell, \ell + 1), \\ 0 & \text{for all other } x, \end{cases} \quad (2.2)$$

where bar is the complex conjugation, and $\ell \geq 0$ is the half-distance between the two elements (in order to shorten the discussion, in what follows we will use term “gain-to-loss distance” for ℓ); the case $\ell = 0$ corresponds to the adjacent elements. Potential $V(x)$ satisfies the standard condition of \mathcal{PT} symmetry: $V(x) = \overline{V}(-x)$. In figure 1 we show a schematics of the potential consisting of an active (“gain”) and absorptive (“losses”) elements.

Spectral singularities, finite-width resonances, and eigenvalues are associated with non-trivial solutions $\psi(x)$ of equation (2.1) with the following behavior at infinity:

$$\psi(x) = C_- e^{ikx}, \quad \text{for } x < -\ell - 1, \quad \text{and} \quad \psi(x) = C_+ e^{-ikx}, \quad \text{for } x > \ell + 1, \quad (2.3)$$

where C_+ and C_- are constants. Values of k in the upper complex half-plane, $\text{Im } k > 0$, are associated with exponentially growing generalized eigenfunctions which in the scattering theory correspond to finite-width resonances. The case $\text{Im } k = 0$ corresponds to spectral singularities, i.e. to the zero-width resonances inside the continuous spectrum, i.e. at $\lambda = k^2 \geq 0$ [1]. Positive and negative k correspond to the coherent perfect absorber (antilaser) and laser solutions, respectively. Values of k in the lower complex half-plane, $\text{Im } k < 0$, correspond to discrete eigenvalues associated with spatially localized bound states.

Equations (2.1)–(2.2) with condition (2.3) can be solved as

$$\begin{aligned} \psi(x, \ell) &= e^{ik(x+\ell+1)}, & x < -\ell - 1, & \quad \psi(x, \ell) = \psi_-(x + \ell), & -\ell - 1 < x < -\ell, \\ \psi(x, \ell) &= C e^{-ik(x-\ell-1)}, & x > \ell + 1, & \quad \psi(x, \ell) = C \psi_+(x - \ell), & \ell < x < \ell + 1, \end{aligned}$$

where C is some constant and functions ψ_- and ψ_+ describe the solution inside the active and absorptive cells; their specific shapes are determined by function W and are independent of ℓ . The requirement of

the continuity of the wave function $\psi(x)$ and of its derivative implies that $\psi_-(-1) = 1$, $\psi'_-(-1) = ik$, $\psi_+(1) = 1$, and $\psi'_+(1) = -ik$.

In the central region, the requirement of continuity of ψ and ψ' implies that for $|x| < \ell$ the solution has the form

$$\psi(x) = \psi_-(0) \cos k(x + \ell) + \psi'_-(0) \frac{\sin k(x + \ell)}{k}. \quad (2.4)$$

At the same time, the solution for $|x| < \ell$ can be also represented as

$$\psi(x) = C\psi_+(0) \cos k(x - \ell) + C\psi'_+(0) \frac{\sin k(x - \ell)}{k}. \quad (2.5)$$

Equations (2.4) and (2.5) are compatible only if k solves the equation

$$(\psi'_-(0) + ik\psi_-(0))(\psi'_+(0) - ik\psi_+(0)) = e^{-4ik\ell}(\psi'_+(0) + ik\psi_+(0))(\psi'_-(0) - ik\psi_-(0)). \quad (2.6)$$

The values $\psi_-(0)$, $\psi'_-(0)$, $\psi_+(0)$, $\psi'_+(0)$ are independent of ℓ . This means that the gain-to-loss distance ℓ enters the main equation (2.6) only in the exponential term $e^{-4ik\ell}$, which is periodic in ℓ . This observation which will be used in what follows.

2.2 Generalized \mathcal{PT} -symmetric step function

The simplest implementation of potential (2.2), which will be considered in the rest of this paper, corresponds to the case when $W(x)$ is a rectangular function with a purely imaginary amplitude, i.e. $W(x) = i\gamma$ for $x \in (0, 1)$ and $W(x) = 0$ outside this interval. Then $\gamma > 0$ is the gain-and-loss amplitude, which determines the gain strength for the left rectangle and the absorption rate for the right rectangle. The resulting potential $V(x)$ is a generalization of the \mathcal{PT} -symmetric step function with adjacent gain and loss regions, which corresponds to $\ell = 0$ and was considered earlier in [1, 6, 45, 46, 51]. In the present paper, we are concerned with the effect of the nonzero gain-to-losses distance $\ell > 0$. The obtained generalized \mathcal{PT} -symmetric step potential can be of relevance in various physical settings. First, it arises in the study of the scattering of TE electromagnetic waves in a rectangular waveguide containing gain and losses such that the complex-valued dielectric permittivity changes along the direction of the propagation. This can be implemented by filling regions of the waveguide with resonant atoms [1, 6] (the gain and loss media are separated by vacuum in order to create nonzero distance ℓ). Another well-established setting, where \mathcal{PT} -symmetric potential (2.2) can arise, corresponds to the propagation of a paraxial optical beam in a system of coupled waveguides with gain and losses [7, 8]. In this case the variation of complex-valued dielectric permittivity takes place in the transverse direction, while the beam propagates in the longitudinal direction. Similar bicentric \mathcal{PT} -symmetric potentials (but in the idealized double-delta function form) have been also considered in the theory of Bose-Einstein condensates, where the domains with gain and losses correspond to the pump and absorption of particles, respectively [52, 53].

For the generalized \mathcal{PT} -symmetric step potential, functions ψ_- and ψ_+ can be evaluated easily:

$$\psi_-(x) = \cos \sqrt{k^2 - i\gamma}(x + 1) + ik \frac{\sin \sqrt{k^2 - i\gamma}(x + 1)}{\sqrt{k^2 - i\gamma}}, \quad -1 < x < 0, \quad (2.7)$$

$$\psi_+(x) = \cos \sqrt{k^2 + i\gamma}(x - 1) - ik \frac{\sin \sqrt{k^2 + i\gamma}(x - 1)}{\sqrt{k^2 + i\gamma}}, \quad 0 < x < 1. \quad (2.8)$$

Using these formulae to compute $\psi_-(0)$, $\psi'_-(0)$, $\psi_+(0)$, $\psi'_+(0)$ and substituting the latter into equation (2.6), we arrive at a final equation for k :

$$F(k, \ell, \gamma) = 0, \quad F(k, \ell, \gamma) := F_-(k, \gamma)F_+(k, \gamma) - e^{-4ik\ell}F_0(k, \gamma), \quad (2.9)$$

$$F_{\pm}(k, \gamma) := 2ik \cos \sqrt{k^2 \pm i\gamma} - (2k^2 \pm i\gamma) \frac{\sin \sqrt{k^2 \pm i\gamma}}{\sqrt{k^2 \pm i\gamma}}, \quad F_0(k, \gamma) := \gamma^2 \frac{\sin \sqrt{k^2 - i\gamma}}{\sqrt{k^2 - i\gamma}} \frac{\sin \sqrt{k^2 + i\gamma}}{\sqrt{k^2 + i\gamma}}.$$

Our next step is a detailed study of the zeroes of function F .

3 Auxiliary lemmata

In this section we point out some obvious properties of the zeroes of the function F defined in (2.9) and prove several auxiliary lemmata. These will be used in the next section to describe a general picture of the zeroes location and their behavior as ℓ and γ vary.

We begin with obvious properties. First, it is straightforward to check that $k = 0$ is zero for all ℓ and γ , that is, $F(0, \ell, \gamma) = 0$, $\ell \geq 0$, $\gamma \geq 0$. Next, we notice that if k is a zero, then $-\bar{k}$ is also a zero, that is, the zeroes of F are symmetric with respect to the imaginary axis. The associated non-trivial solution of equation (2.1) are related by the \mathcal{PT} symmetry transform, i.e. by the combination of spatial reversal $x \mapsto -x$ and the complex conjugation. In particular, for any real root $k > 0$ there always exists the opposite root $-k < 0$, which means that the corresponding spectral singularity is self-dual and associated with the combined laser-antilaser regime.

If k is a zero with a negative imaginary part, then the imaginary part of the corresponding eigenvalue $\lambda = k^2$ does not exceeds γ . Indeed, if ψ is an associated eigenfunction, then due to the equation (2.1) we have

$$\|\psi'\|_{L_2(\mathbb{R})}^2 + (V\psi, \psi)_{L_2(\mathbb{R})} = \lambda \|\psi\|_{L_2(\mathbb{R})}^2,$$

and the inequality $|\operatorname{Im} \lambda| \leq \gamma$ is obtained immediately by taking the imaginary part of this identity. The latter property can be equivalently reformulated as follows: if k is a zero with a negative imaginary part, then

$$|\operatorname{Re} k \operatorname{Im} k| \leq \frac{\gamma}{2}. \quad (3.1)$$

As was already pointed out in Section 2.1, the gain-to-loss distance ℓ enters function F only in the exponent $e^{-4ik\ell}$. This means that if some zero (k_0, ℓ_0, γ_0) of function F is found with real k_0 , then one can immediately generate a sequence of distances

$$\ell_n = \ell_0 + \frac{n\pi}{2k_0}, \quad (3.2)$$

which also correspond to zeros of function F with the same k_0 and γ_0 . In equation (3.2), n is any integer such that $\ell_n \geq 0$.

We proceed to auxiliary lemmata. The first lemma describes the existence and the number of the zeroes.

Lemma 1. *For each $\gamma \geq 0$, $\ell \geq 0$, the function $F(\cdot, \ell, \gamma)$ is holomorphic in the entire complex plane, i.e. it is entire. For each $\gamma > 0$, $\ell \geq 0$, this function has countably many complex zeroes accumulating at infinity only. These zeroes are continuous in ℓ and γ .*

Proof. We represent the sine and cosine functions in the definitions of F_{\pm} , F_0 by their Taylor series. Then we see that the final expansion does not involve square roots but only the integer powers of k . Hence, the function $F(\cdot, \ell, \gamma)$ is entire.

The function $F(k, \ell, \gamma)$ satisfies the estimate $|F(k, \gamma)| \leq e^{C|k|}$ for some fixed constant C and therefore, this is an entire function of order 1. It is clear that as $\gamma > 0$, for each constant $a \in \mathbb{C}$, the function $e^{-ak}F(k, \gamma)$ is not a polynomial in k . Then, by the Hadamard theorem [54, Sect. 4.2, Thm. 4.1], the function $F(\cdot, \gamma)$ has countably many zeroes accumulating at infinity only. The continuity of these zeroes on ℓ and γ is thanks to the smoothness of F . The proof is complete. \square

Remark 1. *As we have showed in the above proof, the choice of the square root in the definition of F_{\pm} is not important. The only restriction is that in the quotients $\frac{\sin \sqrt{k^2 \pm i\gamma}}{\sqrt{k^2 \pm i\gamma}}$ the branch should be the same.*

Remark 2. *As $\gamma = 0$, the function F becomes very simple: $F(k, \ell, 0) = -4k^2 e^{2ik\ell}$ and it has the only zero $k = 0$ of second order. The associated nontrivial solution of equation (2.1) is constant: $\psi(x) \equiv 1$.*

The second lemma is devoted to the case of small γ .

Lemma 2. *As γ is small enough, for each $\ell \geq 0$, there are exactly two zeroes of F satisfying $|k| \leq 2\sqrt{\gamma}$. One of these zeroes is $k = 0$ for all ℓ and γ , while the other is pure imaginary and depends holomorphically on γ and ℓ . The leading terms of its Taylor series are as follows:*

$$k(\gamma, \ell) = i \left(\ell + \frac{1}{3} \right) \gamma + i \left(2\ell^3 + \frac{8}{3}\ell^2 + \frac{53}{45}\ell + \frac{53}{315} \right) \gamma^4 + O(\gamma^6). \quad (3.3)$$

Proof. According to Remark 2, for $\gamma = 0$, the function F has the only zero of second order. Since this function depends continuously on γ , by the Rouché theorem we immediately infer that the function F has exactly two zeroes (counting orders) converging to $k = 0$ as $\gamma \rightarrow 0$. It is easy to confirm that $F(0, \ell, \gamma) = 0$ for all ℓ and γ and hence, $k = 0$ is one of the mentioned zeroes. The other zero is pure imaginary since all zeroes are symmetric with respect to the imaginary axis.

The function $G(k, \ell, \gamma) := k^{-1}F(k, \ell, \gamma)$ is jointly holomorphic in k, ℓ, γ and by straightforward calculations we confirm that

$$G(k, \ell, \gamma) = 4i \left(\ell + \frac{1}{3} \right) \gamma^2 - 4k + O(\gamma^3 + k\gamma), \quad G(0, \ell, 0) = 0, \quad \frac{\partial G}{\partial k}(0, \ell, 0) = -4 \neq 0, \quad (3.4)$$

Then by the inverse function theorem we conclude that there exists the unique zero $k(\ell, \gamma)$ of G in the circle $|k| \leq 2\sqrt{\gamma}$. This zero converges to $k = 0$ as $\gamma \rightarrow 0$ and is jointly holomorphic in ℓ and γ for sufficiently small γ . As (3.4) suggests, this zero is of order $O(\gamma^2)$ as $\gamma \rightarrow 0$. We write the leading terms of its Taylor series

$$k(\ell, \gamma) = c_2\gamma^2 + c_3\gamma^3 + c_4\gamma^4 + c_5\gamma^5 + O(\gamma^6), \quad (3.5)$$

substitute this expression into the equation $G(k, \ell, \gamma) = 0$, expand the result into power series in γ and equate the coefficients at the like powers of ε . This determines the coefficients c_j in (3.5) and a final form of this formula is exactly (3.3). The proof is complete. \square

The next lemma provides a rough information on the location of the zeroes of the function $F(k, \ell, \gamma)$.

Lemma 3. *For each $\gamma > 0$, $\ell \geq 0$, all zeroes of $F(\cdot, \ell, \gamma)$ are located in the domain*

$$\left\{ k : |k| > \sqrt{\gamma}r, \operatorname{Im} k > 0, \sqrt{\gamma}e^{(\ell+1)\operatorname{Im} k} < |k| < \frac{47}{25}\sqrt{\gamma}e^{(\ell+1)\operatorname{Im} k}, |k| < \frac{76}{73}\gamma e^{(\ell+\frac{9}{8})|k|} \right\} \cup \left\{ k : |k| \leq \sqrt{\gamma}r \right\},$$

where

$$r := \max \left\{ \frac{39}{20}, \frac{\sqrt{\gamma}}{2} \right\}. \quad (3.6)$$

If γ is small enough, the function F has no zeroes in the lower complex half-plane.

Proof. Let k be a zero of F and denote $z := k\mu^{-1}$, $\mu := \sqrt{\gamma}$. By routine straightforward calculations we confirm that z solves the equation

$$\begin{aligned} Q(z, \ell, \mu) &= 0, \quad Q(z, \ell, \mu) := Q_1(z, \mu) - Q_2(z, \ell, \mu), \\ Q_1(z, \mu) &:= \left((z + \sqrt{z^2 - i})^2 + \frac{e^{-2i\mu\sqrt{z^2 - i}}}{(z + \sqrt{z^2 - i})^2} \right) \left((z + \sqrt{z^2 + i})^2 + \frac{e^{-2i\mu\sqrt{z^2 + i}}}{(z + \sqrt{z^2 + i})^2} \right), \\ Q_2(z, \ell, \mu) &:= e^{-4i\mu\ell z} (1 - e^{-2i\mu\sqrt{z^2 - i}}) (1 - e^{-2i\mu\sqrt{z^2 + i}}). \end{aligned}$$

Consider z obeying the restrictions $|z| \geq r \geq \frac{17}{10}$, $\operatorname{Im} z \leq 0$ and denote $r_1 := (r + \sqrt{r^2 - 1})^{-1}$. Then

$$\begin{aligned} z + \sqrt{z^2 \pm i} &= 2z \left(1 \pm \frac{i}{z^2} \frac{1}{1 + \sqrt{1 \pm iz^{-2}}} \right), \quad \sqrt{z^2 \pm i} - z = \pm \frac{i}{z} \frac{1}{1 + \sqrt{1 \pm iz^{-2}}}, \\ |1 + \sqrt{1 \pm iz^{-2}}| &\geq 1 + \sqrt{1 - r^{-2}} \geq 1, \quad |\sqrt{z^2 \pm i} - z| \leq r_1, \\ |z + \sqrt{z^2 \pm i}| &\geq 2|z| \left(1 - \frac{r_1}{r} \right) = 2|z| \frac{\sqrt{r^2 - 1}}{r} \geq 2\sqrt{r^2 - 1}. \end{aligned} \quad (3.7)$$

These inequalities allow us to estimate the functions Q_1, Q_2 :

$$\begin{aligned} |Q_1(z, \mu)| &\geq \left(\frac{4(r^2 - 1)}{r^2} |z|^2 - \frac{e^{2\mu(\text{Im } z + r_1)}}{4(r^2 - 1)} \right)^2 \geq \left(4(r^2 - 1) - \frac{e^{2\mu r_1}}{4(r^2 - 1)} \right)^2, \\ |Q_2(z, \ell, \mu)| &\leq e^{4\mu \ell \text{Im } z} \left(1 + e^{2\mu(\text{Im } z + r_1)} \right)^2 \leq \left(1 + e^{2\mu r_1} \right)^2, \end{aligned} \quad (3.8)$$

Since $r \geq \frac{39}{20}$, $r \geq \frac{\mu}{2}$, we have $4(r^2 - 1) \geq \rho_0 := \frac{1121}{100}$, $e^{2\mu r_1} \leq e^{\frac{156}{39 + \sqrt{1121}}}$ and

$$|Q(z, \ell, \mu)| \geq |Q_1(z, \ell, \mu)| - |Q_2(z, \ell, \mu)| \geq \left(\frac{1121}{100} - \frac{100}{1121} e^{\frac{156}{39 + \sqrt{1121}}} \right)^2 - \left(1 + e^{\frac{156}{39 + \sqrt{1121}}} \right)^2 > 16 > 0.$$

Hence, for the considered values of z , we have $|Q(z, \ell, \mu)| > 0$ and such z can not be a zero of Q .

Let $|z| > r$, $\text{Im } z > 0$. Then it follows from (3.8) that

$$|Q(z, \ell, \mu)| \geq \left(\frac{4484}{1521} |z|^2 - \frac{96}{125} e^{2\mu \text{Im } z} \right)^2 - 93 e^{4\mu(\ell+1) \text{Im } z}$$

and the function Q is non-zero provided $|z| > \frac{47}{25} e^{\mu(\ell+1) \text{Im } z}$. Assume now that $e^{(\ell+1)\mu \text{Im } z} \geq |z|$, $\text{Im } z > 0$, $|z| > r$. In the same way as above we estimate

$$\begin{aligned} |Q(z, \ell, \mu)| &\geq e^{4\mu \ell \text{Im } z} \left(e^{2\mu(\text{Im } z + r_1)} - 1 \right)^2 - \left(4|z|^2 \left(1 + \frac{r_1}{r} \right)^2 + \frac{e^{2\mu(\text{Im } z + r_1)}}{4(r^2 - 1)} \right)^2 \\ &\geq 57.827 e^{4\mu(\ell+1) \text{Im } z} - (5.213|z|^2 + 0.768 e^{2\mu \text{Im } z})^2 > 59 e^{4\mu(\ell+1) \text{Im } z} - 55|z|^4 \geq 0 \end{aligned}$$

and the function $Q(z, \ell, \mu)$ is again non-zero.

Consider z obeying $|z| \geq r$, $\text{Im } z > 0$. Employing the estimate $\sinh t \leq t \cosh t$, $t \geq 0$, by straightforward calculations for all $w = w_1 + iw_2 \in \mathbb{C}$ we check that

$$|e^w - 1|^2 = 4e^{w_1} \left(\sinh^2 \frac{w_1}{2} + \sin^2 w_2 \right) \leq \frac{w_1^2}{4} (e^{w_1} + 1)^2 + w_2^2 \leq \frac{7|w|^2 e^{2|w|}}{4}.$$

Hence,

$$|e^{-2i\mu\sqrt{z^2 \pm i}} - 1| \leq \sqrt{7}\mu\sqrt{|z|^2 + 1} e^{\mu\sqrt{|z|^2 + 1}} \leq \sqrt{7(1 + r^{-2})}\mu|z| e^{\mu\sqrt{|z|^2 + 1}}.$$

Rewriting the exponents in the functions Q_1, Q_2 as $e^{-2i\mu\sqrt{z^2 \pm i}} = 1 + (e^{-2i\mu\sqrt{z^2 \pm i}} - 1)$, by (3.7) we get

$$|Q(z, \ell, \mu)| \geq \left(\frac{73}{25} |z|^2 - \frac{8}{125} \mu |z| e^{\frac{9}{8}\mu|z|} \right)^2 - \frac{177}{20} \mu^2 |z|^2 e^{(4\ell + \frac{9}{4})\mu|z|} > 0 \quad \text{as} \quad |z| \geq \frac{76}{73} \mu e^{(2\ell + \frac{9}{8})\mu|z|}.$$

Assume that γ is small enough. Then according Lemma 2, the function F has only two zeroes in the circle $|k| \leq 2\sqrt{\gamma}$, one of them is $k = 0$, while the other is located in the upper half-plane. \square

In what follows, given a set S , by \overline{S} we denote the closure of this set, while for a number z , the symbol \bar{z} stands for the complex conjugation.

The next lemmata describe the behavior the zeroes as ℓ grows.

Lemma 4. *Let $\gamma \neq 0$. For each $n \in \mathbb{Z}$ obeying the estimate*

$$\frac{\pi|n|}{2} + \frac{\pi}{4} \leq \Theta(\gamma)\ell, \quad \Theta(\gamma) := \frac{2(1 - e^{-\frac{\pi}{4}})\gamma}{17(1 + \sqrt{1 - e^{-\frac{\pi}{4}}})\sqrt{\gamma} + \frac{10\pi}{\sqrt{3}}}, \quad (3.9)$$

the circle $\{k : |k - \frac{\pi n}{2\ell}| < \frac{\pi}{4\ell}\}$ contains exactly one simple zero $k_n(\ell, \gamma)$ of equation (2.9). This zero is holomorphic in ℓ^{-1} and as $\ell \rightarrow +\infty$, the leading terms of its Taylor series are

$$k_n(\ell, \gamma) = \frac{\pi n}{2} \ell^{-1} - \frac{\sqrt{2\pi n}(\sinh \sqrt{2\gamma} - \sin \sqrt{2\gamma})}{4\sqrt{\gamma}(\cosh \sqrt{2\gamma} - \cos \sqrt{2\gamma})} \ell^{-2} - \frac{i\pi^2 n^2 \sinh \sqrt{2\gamma} \sin \sqrt{2\gamma} - 2\pi n(\sinh \sqrt{2\gamma} - \sin \sqrt{2\gamma})^2}{\gamma(\cosh \sqrt{2\gamma} - \cos \sqrt{2\gamma})^2} \ell^{-3} + O(\ell^{-4}). \quad (3.10)$$

Proof. We divide equation (2.9) by $\frac{\sin \sqrt{k^2 - i\gamma}}{\sqrt{k^2 - i\gamma}} \frac{\sin \sqrt{k^2 + i\gamma}}{\sqrt{k^2 + i\gamma}}$ and rewrite it as

$$1 - e^{-4ik\ell} + k\gamma^{-1}F_1(k, \gamma) + k^2\gamma^{-2}F_2(k, \gamma) = 0, \quad (3.11)$$

$$F_1(k, \gamma) := 2 \left(\cos \sqrt{k^2 + i\gamma} \frac{\sqrt{k^2 - i\gamma}}{\sin \sqrt{k^2 - i\gamma}} - \cos \sqrt{k^2 - i\gamma} \frac{\sqrt{k^2 + i\gamma}}{\sin \sqrt{k^2 + i\gamma}} \right),$$

$$F_2(k, \gamma) := -4(\sqrt{k^2 - i\gamma} \cot \sqrt{k^2 - i\gamma} - ik)(\sqrt{k^2 + i\gamma} \cot \sqrt{k^2 + i\gamma} - ik).$$

Denote $\Pi := \{k : |k| < \frac{\pi}{4\sqrt{3}}\}$. We first estimate the functions F_1 and F_2 by obtaining appropriate bounds for each term in their definitions. Since $\sqrt{k^2 - i\gamma} = \sqrt{k^2} + i\gamma$,

$$\max_{k \in \Pi} |\sqrt{k^2 + i\gamma} \cot \sqrt{k^2 + i\gamma}| = \max_{k \in \Pi} |\sqrt{k^2 - i\gamma} \cot \sqrt{k^2 - i\gamma}| = \max_{k \in \Pi} \left| \sqrt{k^2 - i\gamma} \frac{\cos \sqrt{k^2 \pm i\gamma}}{\sin \sqrt{k^2 \mp i\gamma}} \right| \quad (3.12)$$

and it is sufficient to estimate the first maximum only.

Consider first the values $\gamma \leq \frac{\pi^2}{24}$. Then $\{\sqrt{k^2 + i\gamma} : k \in \Pi\} \subset \Pi^{(1)} := \{z : |z| \leq \frac{\pi}{4}\}$. Hence, the function $k \mapsto \sqrt{k^2 + i\gamma} \cot \sqrt{k^2 + i\gamma}$ is holomorphic on $\overline{\Pi^{(1)}}$ and by the maximum modulus principle,

$$\max_{k \in \Pi} |\sqrt{k^2 + i\gamma} \cot \sqrt{k^2 + i\gamma}| < \left(\max_{z \in \partial \Pi^{(1)}} |z|^2 \frac{|\cosh z|^2}{|\sinh z|^2} \right)^{\frac{1}{2}}. \quad (3.13)$$

For $z \in \partial \Pi^{(1)}$ we let $z = \frac{\pi}{4}e^{it}$, $t \in [0, 2\pi)$, and employing the estimates

$$\sinh y \geq y, \quad y \in [0, +\infty), \quad \sin y \geq \frac{2\sqrt{2}}{\pi}y, \quad y \in \left[0, \frac{\pi}{4}\right], \quad \cos y \leq 1 - \frac{4}{\pi^2}y^2, \quad y \in \left[0, \frac{\pi}{2}\right],$$

by straightforward calculations we get

$$\begin{aligned} \max_{z \in \partial \Pi^{(1)}} |z|^2 \frac{|\cos z|^2}{|\sin z|^2} &= \frac{\pi^2}{16} \max_{t \in [0, \frac{\pi}{2})} \left(1 + \frac{\cos(\frac{\pi}{2} \cos t)}{\sinh^2(\frac{\pi}{4} \sin t) + \sin^2(\frac{\pi}{4} \cos t)} \right) \\ &\leq \frac{\pi^2}{16} \max_{t \in [0, \frac{\pi}{2})} \left(1 + \frac{\sin^2 t}{\sinh^2(\frac{\pi}{4} \sin t) + \frac{1}{2} \cos^2 t} \right) = \frac{\pi^2}{16 \sinh^2 \frac{\pi}{4}}. \end{aligned} \quad (3.14)$$

We proceed to the case $\gamma > \frac{\pi^2}{24}$. Here the set $\{k^2 + i\gamma : k \in \Pi\}$ is the circle of radius $\frac{\pi^2}{48}$ centered at $i\gamma$ and hence,

$$\begin{aligned} \{\sqrt{k^2 + i\gamma} : k \in \Pi\} &\subset \left\{ z : \sqrt{\gamma - \frac{\pi^2}{48}} < |z| < \sqrt{\gamma + \frac{\pi^2}{48}}, \right. \\ &\quad \left. \frac{\pi}{24} < \frac{\pi}{8} - \frac{1}{2} \arcsin \frac{\pi^2}{48\gamma} < \arg z < \frac{\pi}{8} + \frac{1}{2} \arcsin \frac{\pi^2}{48\gamma} < \frac{5\pi}{24} \right\} \subset \Pi^{(2)} \\ \Pi^{(2)} &:= \left\{ z : \sqrt{\gamma - \frac{\pi^2}{48}} \cos \frac{5\pi}{24} < \operatorname{Re} z < \sqrt{\gamma + \frac{\pi^2}{48}} \cos \frac{\pi}{24}, \sqrt{\gamma - \frac{\pi^2}{48}} \sin \frac{\pi}{24} < \operatorname{Im} z < \sqrt{\gamma + \frac{\pi^2}{48}} \sin \frac{5\pi}{24} \right\}. \end{aligned}$$

Again by the maximal modulus principle we get:

$$\begin{aligned} \max_{k \in \Pi} |\sqrt{k^2 + i\gamma} \cot \sqrt{k^2 + i\gamma}| &= \sqrt{\gamma + \frac{\pi^2}{48}} \left(\max_{z_1 + iz_2 \in \Pi^{(2)}} \frac{\cosh 2z_2 + \cos 2z_1}{\cosh 2z_2 - \cos 2z_1} \right)^{\frac{1}{2}} \\ &\leq \sqrt{\gamma + \frac{\pi^2}{48}} \left(\max_{z_1 + iz_2 \in \Pi^{(2)}} \frac{\cosh 2z_2 + 1}{\cosh 2z_2 - 1} \right)^{\frac{1}{2}} = \sqrt{\gamma + \frac{\pi^2}{48}} \left(\frac{\cosh 2\sqrt{\gamma - \frac{\pi^2}{48}} \sin \frac{\pi}{24} - 1}{\cosh 2\sqrt{\gamma - \frac{\pi^2}{48}} \sin \frac{\pi}{24} + 1} \right)^{\frac{1}{2}}. \end{aligned}$$

This estimate and (3.12), (3.13), (3.14) yield:

$$\max_{k \in \Pi} |F_1(k, \gamma)| \leq 17\sqrt{\gamma + \frac{\pi^2}{48}}, \quad \max_{k \in \Pi} |F_2(k, \gamma)| \leq \frac{1}{4} \left(17\sqrt{\gamma + \frac{\pi^2}{48}} + \frac{\pi}{\sqrt{3}} \right)^2.$$

Employing these inequalities, by straightforward calculations we check that

$$|k\gamma^{-1}F_1(k, \gamma) + k^2\gamma^{-2}F_2(k, \gamma)| < 1 - e^{-\frac{\pi}{4}} \quad \text{as} \quad |k| \leq \Theta(\gamma). \quad (3.15)$$

We choose $n \in \mathbb{Z}$ obeying (3.9) and denote $\Pi_n := \{k : |k - \frac{\pi n}{2\ell}| < \frac{\pi}{4\ell}\}$. In each Π_n , the function $k \mapsto 1 - e^{-4ik\ell}$ has the only zero $k = \frac{\pi n}{2\ell}$ and this zero is simple. It is straightforward to check that for $k \in \Pi_n$ the identities hold: $\min_{k \in \partial \Pi_n} |1 - e^{-4ik\ell}| = \min_{|z|=1} |1 - e^{\frac{\pi}{4}z}| = 1 - e^{-\frac{\pi}{4}}$. As $k \in \partial \Pi_n$, estimate (3.15) is also satisfied, and by Rouché theorem equation (3.11) possesses the only zero in Π_n . We denote this root by $k_n(\ell, \gamma)$.

Let us find out the asymptotic behavior of k_n as $\ell \rightarrow +\infty$. We denote $\xi := \ell k$, $\varepsilon := \ell^{-1}$, $k = \varepsilon \xi$ and rewrite equation (3.11) as

$$1 - e^{-4i\xi} + 2\varepsilon\gamma^{-1}F_1(\varepsilon\xi, \gamma) + \varepsilon^2\xi^2\gamma^{-2}F_2(\varepsilon\xi, \gamma) = 0. \quad (3.16)$$

This equation has the root $\xi_n(\varepsilon, \gamma) := \varepsilon^{-1}k_n(\ell, \gamma)$ for each n obeying (3.9). The function in its left hand side is jointly holomorphic in ε , ξ and γ and $(1 - e^{-4i\xi})'|_{\xi=\frac{\pi n}{2}} = 4i \neq 0$. Hence, by the inverse function theorem, the root $\xi_n(\varepsilon)$ is jointly holomorphic in ε and γ . We write the leading terms of the Taylor expansion of $\xi_n(\varepsilon, \gamma)$.

$$\xi_n(\varepsilon, \gamma) = \frac{\pi n}{2} + \xi_n^{(1)}(\gamma)\varepsilon + \xi_n^{(2)}(\gamma)\varepsilon^2 + O(\varepsilon^3).$$

We substitute this expansion into equation (3.16), expand the result in ε and equate the coefficients at the like power of ε . This determines the coefficients $\xi_n^{(1)}$, $\xi_n^{(2)}$ and proves (3.10). \square

It is straightforward to confirm that the zeroes of the functions F_{\pm} correspond to the eigenvalues and resonances of equation (2.1) as $V = V_{\pm}$ is a single step function:

$$V_{\pm}(x) := \begin{cases} \pm i\gamma & \text{as } \pm x \in [0, 1], \\ 0 & \text{otherwise.} \end{cases}$$

Lemma 5. *The functions F_{\pm} have countably many zeroes accumulating at infinity only. There are finitely many zeroes of these functions in the lower half-plane and all of them are located in the ball $\{k : |k| < r_0\sqrt{\gamma}\}$, $r_0 := \frac{6}{5} \max\{1, \sqrt{\gamma}\}$. All zeroes of F_{\pm} are simple except a possible zero $k = 2i$. If $k = 2i$ is a zero of F_+ or F_- , it is of the second order. For all $\gamma > 0$, the function F_{\pm} can have at most one real zero, which is negative for F_+ and is positive for F_- .*

Proof. The functions F_{\pm} are entire and this is why they have countably many zeroes accumulating at infinity only. In the same way how estimate (3.8) was proved, we immediately get

$$|F_{\pm}(k, \gamma)| \geq 4(r_0^2 - 1) - \frac{e^{2\sqrt{\gamma}r_2}}{4(r_0^2 - 1)} > 0 \quad \text{as} \quad |k| \geq \sqrt{\gamma}r_0, \quad \text{Im } k \leq 0, \quad r_2 := \left(r_0 + \sqrt{r_0^2 + 1}\right)^{-1}.$$

Hence, all zeroes of F_{\pm} with negative imaginary part are located in the circle $|k| < \sqrt{\gamma}r_0$. Since they accumulate at infinity only, there are only finitely many of them in the aforementioned circle.

Let k be a zero of F_+ . It is clear that $k \neq 0$, $\sqrt{k^2 + i\gamma} \neq 0$. We calculate the first derivative and we see immediately that if $\frac{\partial F_+}{\partial k}(k, \gamma) = 0$, by the equation $F_+(k, \gamma) = 0$ this implies $k = 2i$. Then we calculate the second derivative of F_+ at $k = 2i$ and see that it is nonzero. Hence, all zeroes of F_+ are simple except a possible second order zero at $k = 2i$. The case of F_- is studied in the same way.

To find real zeroes of F_+ , similar to the proof of Lemma 7, for real positive k we make the change

$$k = \frac{\beta}{2}\sqrt{u^{-2} - u^2}, \quad 0 < u < 1, \quad \sqrt{k^2 \pm i\gamma} = \frac{\sqrt{\gamma}}{\sqrt{2}}(u^{-1} \pm iu), \quad i\gamma \pm 2k^2 = \gamma(i \pm u^{-2} \mp u^2). \quad (3.17)$$

Taking then the real and imaginary parts of F_+ and factorizing them, we obtain:

$$\begin{aligned} \left(u^2 \cos \frac{\beta}{2u} - \sqrt{1-u^4} \sin \frac{\beta}{2u}\right) \left(\sinh \frac{\beta u}{2} + \sqrt{1-u^2} \cosh \frac{\beta u}{2}\right) &= 0, \\ \left(u^2 \sin \frac{\beta}{2u} + \sqrt{1-u^4} \cos \frac{\beta}{2u}\right) \left(\cosh \frac{\beta u}{2} + \sqrt{1-u^2} \sinh \frac{\beta u}{2}\right) &= 0. \end{aligned} \quad (3.18)$$

The second factors in the above equations are obviously non-zero and the first ones can not vanish simultaneously since otherwise we would have got $\cos \frac{\beta}{2u} = \sin \frac{\beta}{2u} = 0$. To find negative real zeroes, we make the same change as in (3.17) but with β replaced by $-\beta$. Then we arrive immediately to equations (3.18), where the same replacement is made. Since $\sinh \frac{\beta u}{2} < \cosh \frac{\beta u}{2}$, only the first factor in the second equation can vanish and then only the second factor is the first equation can be zero:

$$\sqrt{1-u^4} \cos \frac{\beta}{2u} - u^2 \sin \frac{\beta}{2u} = 0, \quad \sqrt{1-u^4} = \tanh \frac{\beta u}{2}. \quad (3.19)$$

The function $\sqrt{1-u^4}$, $u \in (0, 1)$, decreases monotonically from 1 to 0, while $\tanh \frac{\beta u}{2}$ increases monotonically from 0 to $\tanh \frac{\beta}{2}$. Hence, the second equation in (3.19) has the unique root. This root solves the first equation only for certain values of β . The zeroes of F_- are studied in the same way. \square

Let $k = K_{\pm}^{(n)}(\gamma)$, $n = 1, \dots, N_{\pm}$, be the zeroes of the functions F_{\pm} in the lower half-plane. According Lemma 5, all of them are simple. Consider the points $K_{\pm}^{(n)}$ on the complex plane identifying coinciding ones. Let d be the minimal among the mutual distances between these points and the distances from them to the real axis. We introduce the constants:

$$\begin{aligned} C_1 &:= \gamma^2 + (1+r^2)^{-1} \sinh^2 \sqrt{(1+r^2)\gamma}, & C_2 &:= \inf_{\substack{|\operatorname{Re} k| \leq \sqrt{\gamma}r, \\ -\frac{d}{2} < \operatorname{Im} k < 0}} |F_-(k, \gamma)F_+(k, \gamma)| |\operatorname{Im} k|^{-2}, \\ C_3 &:= \min_{\substack{|k| = \sqrt{\gamma}r, \\ \operatorname{Im} k \leq 0}} |F_-(k, \gamma)F_+(k, \gamma)|, & C_4 &:= \min_n \min_{|k - K_{\pm}^{(n)}| \leq \frac{d}{2}} |F_-(k, \gamma)F_+(k, \gamma)| |k - K_{\pm}^{(n)}|^{-2}. \end{aligned}$$

Lemma 6. *As*

$$\ell > \frac{\sqrt{C_2}}{\sqrt{C_1}} \max \left\{ 1, \left(\frac{C_1}{C_3} \right)^{\frac{1-\ln 2}{2}} \right\}, \quad \frac{\ln \frac{\ell \sqrt{C_1}}{\sqrt{C_2}}}{2(1-\ln 2)\ell} \leq \frac{d}{2}, \quad (3.20)$$

the function F has exactly $N_- + N_+$ zeroes $k^{(n)}(\ell, \gamma)$, $n = 1, \dots, N_{\pm}$, counting their orders in the half-plane

$$\operatorname{Im} k \leq -\frac{\ln \frac{\ell \sqrt{C_1}}{\sqrt{C_2}}}{2(1-\ln 2)\ell}.$$

The constant C_4 is positive and for ℓ obeying (3.20) and

$$\ell > \frac{1}{2 \operatorname{Im} K_{\pm}^{(n)} + d} \ln \frac{2\sqrt{C_1}}{d\sqrt{C_4}}, \quad (3.21)$$

the estimates hold:

$$|k_{\pm}^{(n)}(\ell, \gamma) - K_{\pm}^{(n)}(\gamma)| < \frac{\sqrt{C_1}}{\sqrt{C_4}} e^{(2 \operatorname{Im} K_{\pm}^{(n)} + d)\ell}. \quad (3.22)$$

Proof. We begin with the estimate

$$\gamma^2 \left| \frac{\sin \sqrt{k^2 - i\gamma}}{\sqrt{k^2 - i\gamma}} \frac{\sin \sqrt{k^2 + i\gamma}}{\sqrt{k^2 + i\gamma}} \right| \leq C_1 \quad \text{as} \quad |k| \leq \sqrt{\gamma}r, \quad \operatorname{Im} k \leq 0, \quad (3.23)$$

which can be checked by straightforward calculations employing the maximum modulus principle. According to Lemma 3, all zeroes of the function F below the line $\operatorname{Im} k = -\frac{\ln \frac{\ell \sqrt{C_1}}{\sqrt{C_2}}}{2(1 - \ln 2)\ell}$ also obey $|k| < \sqrt{\gamma}r$ and therefore, they are contained in

$$\Pi := \left\{ k : |k| < \sqrt{\gamma}r, \operatorname{Im} k < -\frac{\ln \frac{\ell \sqrt{C_1}}{\sqrt{C_2}}}{2(1 - \ln 2)\ell} \right\}.$$

As $k \in \partial\Pi$, by the definition of constants C_i , $i = 1, \dots, 4$, and (3.20), (3.23), the inequalities

$$|F_-(k, \gamma)F_+(k, \gamma)| \geq \min \left\{ \frac{C_2 \ln^2 \frac{\ell \sqrt{C_1}}{\sqrt{C_2}}}{4(1 - \ln 2)^2 \ell^2}, C_3 \right\} > \max_{\Pi} \gamma^2 \left| e^{-4ik\ell} \frac{\sin \sqrt{k^2 - i\gamma}}{\sqrt{k^2 - i\gamma}} \frac{\sin \sqrt{k^2 + i\gamma}}{\sqrt{k^2 + i\gamma}} \right|$$

hold. Hence, by the Rouché theorem we immediately conclude that the function F has the same amount of zeroes inside Π as the function F_-F_+ does and this proves the first part of the lemma.

The constant C_4 is non-zero since the functions F_{\pm} has a simple zero at $K_{\pm}^{(n)}$ and the function F_-F_+ has also simple zeroes at $K_{\pm}^{(n)}$ if $K_-^{(n)} \neq K_+^{(n)}$ and a second order zero if $K_-^{(n)} = K_+^{(n)}$. Then by inequalities (3.23) and the definition of the constant C_4 we infer that, as

$$|k - K_{\pm}^{(n)}| = \rho := \frac{\sqrt{C_1}}{\sqrt{C_4}} e^{-(2 \operatorname{Im} K_{\pm}^{(n)} - d)\ell} < \frac{d}{2}$$

and ℓ obeys (3.20), (3.21), the estimates

$$|F_-(k, \gamma)F_+(k, \gamma)| \geq C_4 \rho^2, \quad \gamma^2 \left| e^{-4ik\ell} \frac{\sin \sqrt{k^2 - i\gamma}}{\sqrt{k^2 - i\gamma}} \frac{\sin \sqrt{k^2 + i\gamma}}{\sqrt{k^2 + i\gamma}} \right| \leq C_1 e^{(4 \operatorname{Im} K_{\pm}^{(n)} + 2d)\ell} < C_4 \rho^2$$

are valid. Hence, we can apply the Rouché theorem to the function F and we conclude that this function has the same amount of zeroes inside the circle $\{k : |k - K_{\pm}^{(n)}| < \rho\}$ as the functions F_-F_+ does. This implies estimates (3.22). \square

Finally, we prove the absence of pure imaginary zeroes in the lower complex half-plane, which means that the waveguide does not have real discrete eigenvalues $\lambda < 0$.

Lemma 7. *Equation (2.9) has no pure imaginary zeroes in the lower complex half-plane.*

Proof. For negative pure imaginary k we make the change

$$k = -\frac{i\beta}{2} \sqrt{u^{-2} - u^2}, \quad 0 < u < 1, \quad \sqrt{k^2 \pm i\gamma} = \frac{\beta}{2}(iu^{-1} \pm u), \quad i\gamma \pm 2k^2 = \frac{\beta^2}{2}(i \mp u^{-2} \pm u^2),$$

where $\beta := \sqrt{2\gamma}$. We multiply equation (2.9) by $\sqrt{k^2 - i\gamma}\sqrt{k^2 + i\gamma}$, substitute the above formulae and divide the result by $\sqrt{1 - u^4}$. This leads us to the equation:

$$u^{-4} \sqrt{1 - u^4} \cosh \beta u^{-1} + \frac{1 - e^{-\frac{2\beta\ell}{u} \sqrt{1 - u^4}}}{2\sqrt{1 - u^4}} (\cosh \beta u^{-1} - \cos \beta u)$$

$$+ u^{-4} \sinh \beta u^{-1} + \sqrt{1 - u^4} \cos \beta u - u^2 \sin \beta u = 0.$$

The first two terms in this equation are non-zero for all u, β, ℓ . Therefore, to prove the lemma, it is sufficient to check that the sum of remaining three terms is non-negative. For $\beta > \operatorname{arcsinh} 1$ we have

$$\begin{aligned} \sqrt{1 - u^4} \cos \beta u - u^2 \sin \beta u &\leq \left(\sqrt{1 - u^4}^2 + u^4 \right)^{\frac{1}{2}} = 1, \\ u^{-4} \sinh \beta u^{-1} + \sqrt{1 - u^4} \cos \beta u - u^2 \sin \beta u &> u^{-4} \sinh \beta u^{-1} - 1 > \sinh \beta - 1 > 0. \end{aligned}$$

As $0 \leq \beta \leq \operatorname{arcsinh} 1 < \frac{\pi}{2}$, by the inequalities $\cos \beta u \geq \cos \beta > 0$, $u^2 \sin \beta u \leq \sin \beta$, $\sinh \beta - \sin \beta \geq 0$, we get

$$u^{-4} \sinh \beta u^{-1} + \sqrt{1 - u^4} \cos \beta u - u^2 \sin \beta u \geq u^{-4} \sinh \beta - \sin \beta \geq \sinh \beta - \sin \beta \geq 0.$$

The proof is complete. \square

4 Behavior of zeroes and ladders of resonances and eigenvalues

In this section we employ the results of the previous section to describe how the zeroes of the function F depend on γ and ℓ .

4.1 Location of zeroes and dependence of gain-and-loss amplitude

According Remark 2, as $\gamma = 0$, there is a single zero $k = 0$. It corresponds to a resonance and the associated solution to equation (2.1) is the constant function. As soon as γ is positive, no matter how small it is, there arise *infinitely many* zeroes of the function F , see Lemma 1, and we still have a resonance at $k = 0$ but now the associated solution of equation (2.1) is non-constant. Despite the potential V is a *regular* perturbation as γ is small, it influences the general spectral picture quite essentially producing at once infinitely many zeroes. All these zeroes are located symmetrically with respect to the imaginary axis and are continuous in γ and ℓ . For the corresponding eigenvalues and resonances given by $\lambda = k^2$, this property means that we deal with complex-conjugate pairs of resonances and eigenvalues, as it is usual for \mathcal{PT} -symmetric systems.

By Lemma 2, for small γ , we have one more pure imaginary zero close to $k = 0$. This zero is holomorphic in γ and the leading terms of its Taylor series are given by (3.3). Since $(\ell + \frac{1}{3})\gamma > 0$, this zero corresponds to a resonance. The corresponding value λ is negative and lies close or next to the bottom of the essential spectrum.

Lemmata 1 and 3 state the following important facts. The zeroes can accumulate at infinity only, that is, each circle of a fixed radius in the complex plane contains only finitely many zeroes. Except for zeroes in the circle $|k| < \sqrt{\gamma}r$, where r is introduced in (3.6), all other zeroes are located in the upper half-plane in the exponential sector

$$\sqrt{\gamma}e^{(\ell+1)\operatorname{Im} k} < |k| < \frac{47}{25}\sqrt{\gamma}e^{(\ell+1)\operatorname{Im} k}, \quad |k| < \frac{76}{73}\gamma e^{(\ell+\frac{9}{8})|k|}.$$

The second inequality deserves a special consideration. Let γ be small enough and consider the zeroes outside the circumference $|k| = \sqrt{\gamma}r$. Then the inequality implies

$$\frac{39}{20} < \frac{76}{73}\gamma^{\frac{1}{2}}e^{(\ell+\frac{9}{8})|k|} \quad \Rightarrow \quad |k| > \frac{1}{\ell + \frac{9}{8}} \ln \frac{2847\gamma^{-\frac{1}{2}}}{1520}$$

and hence, except the zeroes discussed in Lemma 2, all other zeroes are located far from $k = 0$ at distances of order $O(|\ln \gamma|)$. This means that for small γ , infinitely many zeroes emerge from infinity in the upper half-plane and only two of them come from zero and are located in the upper half-plane, too.

Since all zeroes with $\text{Im } k \leq 0$ are located in the aforementioned circle $|k| < \sqrt{\gamma}r$, for all $\gamma > 0$ and $\ell \geq 0$, there are only *finitely many* such zeroes. They correspond to the eigenvalues (bound states), and for them and inequality (3.1) should be satisfied as well. All eigenvalues are complex-valued since according Lemma 7, there are no pure imaginary zeroes in lower complex half-plane. Real zeroes correspond to spectral singularities. Thus, for all $\ell \geq 0$ and $\gamma > 0$ the system has infinitely many resonances and finitely many bound states and spectral singularities. The size of the aforementioned circle, in which the zeroes with $\text{Im } k \leq 0$ are located, increases proportionally to γ (see the definition of r in (3.6)). Hence, by increasing γ we have more chances to get the zeroes in the lower half-plane and as we shall discuss below, this is indeed the case.

4.2 Large distance regime and ladders of eigenvalues and resonances

Here we discuss the behavior of the zeroes as ℓ grows. Lemma 6 states that below the line $\text{Im } k = -\frac{\ln \frac{\ell \sqrt{C_1}}{\sqrt{C_2}}}{2(1-\ln 2)\ell}$, the function F possesses the same number zeroes as the functions F_- and F_+ do and these zeroes of F converge to the zeroes of F_{\pm} as $\ell \rightarrow +\infty$, see (3.22). As $\ell \rightarrow +\infty$, the distance from the aforementioned line to the real axis is of order $O(\ell^{-1} \ln \ell)$ and is small. A natural question whether there can be some other zeroes in the lower half-plane above this line is answered in Lemma 4 and the answer is positive. According to this lemma, making ℓ large enough, we certainly have $2N + 1$ zeroes in the vicinity of the real axis, where $N := \lfloor \frac{1}{2} + \frac{2\Theta(\gamma)}{\pi} \ell \rfloor$, $\lfloor \cdot \rfloor$ is the integer part of a number. All these zeroes are located in the circles $\{k : |k - \frac{\pi n}{2\ell}| < \frac{\pi}{4\ell}\}$, exactly one zero in each circle, and all these circles are inside a fixed circle $\{k : |k| < \Theta(\gamma)\}$. As ℓ grows, the number of such zeroes increases as well but all of them remain in the circle $\{k : |k| < \Theta(\gamma)\}$. As γ grows, the size of the latter circle increases as $O(\sqrt{\gamma})$. For large ℓ , these zeroes are approximately given by asymptotic formulae (3.10). As these formulae show, if $\sin \sqrt{2\gamma} < 0$, the zeroes are located in the upper half-plane and correspond to resonances. The described behavior is similar to that of Wannier-Stark resonances. Namely, for gain-and-loss amplitude we again have a ladder of resonances accumulating in the vicinity certain zone in the essential spectrum. As $\sin \sqrt{2\gamma} > 0$, these zeroes are in the lower half-plane and correspond to eigenvalues. The number of these zeroes guaranteed by Lemma 4 grows as $O(\ell)$ as $\ell \rightarrow +\infty$, while the distances between the neighbouring zeroes are of order $O(\ell^{-1})$. This means that we have either resonances or eigenvalues accumulating to the segment $[-\Theta(\gamma), \Theta(\gamma)]$ on the real axis, see Figure 2(a,b). It is especially interesting to notice that by means of a continuous change of the gain-and-loss amplitude one can transform a ladder of resonances to a ladder of eigenvalues or vice versa as shown in figure 2(b). Such a transformation is obviously not possible for Wannier-Stark ladders in self-adjoint operators where complex eigenvalues can't exist. The peculiar regime $\sin \sqrt{2\gamma} = 0$ corresponds to the situation when the leading order of imaginary part of expansion (3.10) vanishes [curve 2 in figure 2(b)]. A delicate analysis shows that in this case the imaginary parts of zeroes described by Lemma 4 are nonzero and amount to $O(\ell^{-5})$. Thus, for $\sin \sqrt{2\gamma} = 0$ we have a ladder of coexisting “nearly spectral singularities” with extremely small by nevertheless nonzero imaginary parts (genuine spectral singularities with exactly zero imaginary parts will be discussed in section 5).

It is interesting to compare this spectral picture with that in the limiting situation $\ell = +\infty$ and the first issue is which operator are to be regarded as limiting ones. Such limiting operator are to be treated in the norm resolvent sense, that is, we should find an approximation for the resolvent of our operator as $\ell \rightarrow +\infty$. According the results of [21], as $\ell \rightarrow +\infty$, the solution of the equation

$$-u'' + Vu - \lambda u = f \quad \text{in } \mathbb{R}, \quad u \in H^2(\mathbb{R}), \quad f(x) := f_-(x + \ell) + f_0(x) + f_+(x - \ell), \quad f_0, f_{\pm} \in L_2(\mathbb{R}),$$

is approximated in the norm resolvent sense up to a small error by $u_-(x + \ell) + u_0(x) + u_+(x - \ell)$. Here $u_0, u_{\pm} \in H^2(\mathbb{R})$ solve the equations

$$-u_0'' - \lambda u_0 = f_0, \quad -u_{\pm}'' + V_{\pm} u_{\pm} - \lambda u_{\pm} = f_{\pm} \quad \text{in } \mathbb{R},$$

where the potentials V_{\pm} were introduced in (3.17). Hence, the limiting operator is in fact a direct sum of three operators $\mathcal{H}_- \oplus \mathcal{H}_0 \oplus \mathcal{H}_+$, $\mathcal{H}_0 := -\frac{d^2}{dx^2}$, $\mathcal{H}_{\pm} := -\frac{d^2}{dx^2} + V_{\pm}$. The essential spectra of all three

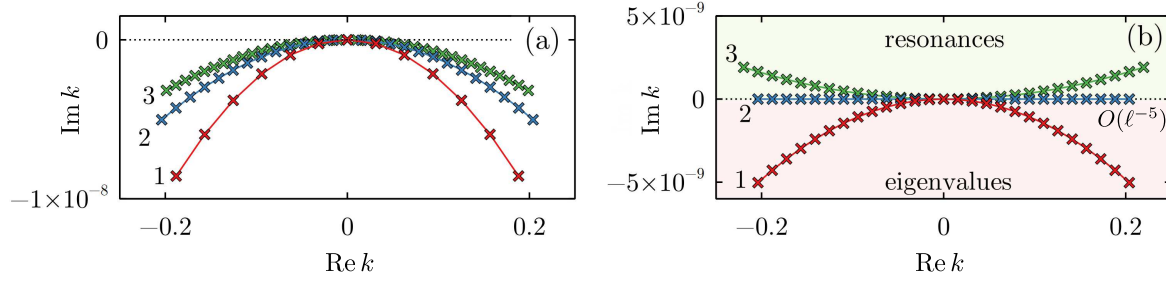


Figure 2: Ladders of zeroes plotted according to the leading terms of expansion (3.10). (a) Accumulation of zeroes (corresponding to eigenvalues) to the segment $[-\Theta(\gamma), \Theta(\gamma)]$ as the gain-to-loss distance ℓ grows. Here the gain-and-loss amplitude $\gamma = 40$ and $\ell = 50$ (curve 1), 100 (curve 2) and 150 (curve 3). The zeroes are shown with crosses; thin solid lines are to guide the eye. (b) Transformation of the ladder of eigenvalues (curve 1) to a ladder of resonances (curve 3) under the change of the gain-and-loss amplitude. Here $\ell = 100$ and $\gamma = 40$ (curve 1) and $\gamma = 50$ (curve 3). Curve 2 corresponds to $\gamma = 9\pi^2/2 \approx 44.413$. In this case the imaginary part of term $\propto \ell^{-3}$ in expansion (3.10) vanishes, and we obtain a ladder of coexisting “nearly spectral singularities” with $\text{Im } k = O(\ell^{-5})$.

operators are $[0, +\infty)$. The operator \mathcal{H}_0 has the only resonance at $k = 0$, while the resonances and the eigenvalues of the operators \mathcal{H}_\pm are expressed via the zeroes of the functions F_\pm by the formula $\lambda = k^2$, see Lemma 5. In view of such approximation, it would be natural to expect that as $\ell \rightarrow +\infty$, the above discussed zeroes $k_n(\ell, \gamma)$ converge to similar real zeroes of the functions F_\pm or to zero. *This is not true!* Indeed, by Lemma 5, each of the functions F_\pm has at most *one* real zero, while the number of the zeroes $k_n(\ell, \gamma)$ in the vicinity of this segment *increases* as $\ell \rightarrow +\infty$. Thus, regarding the case $\ell = +\infty$ and eigenvalues equations for the operators \mathcal{H}_\pm as limiting, for sufficiently large finite ℓ we get a *large number* of *eigenvalues or resonances emerging from internal points* of the zone $[0, \Theta^2(g)]$ in essential spectrum. And at most three points (including zero) are spectral singularities for the limiting equations. In other words, here we have eigenvalues emerging from ordinary points in the essential spectrum not being spectral singularities for the unperturbed operators. And while in the case of Wannier-Stark resonances their existence is due to the eigenvalues of the operator $-\frac{d^2}{dx^2} + \varepsilon x$ accumulating on the real line as $\varepsilon \rightarrow +0$, this surely not the case in our model.

Here we just make one more important observation. The presence of the mentioned zero-width resonances, or real zeroes of F , could be regarded as an explanation or the reason for the existence of the above described ladder of resonances and eigenvalues. However, *this is not the case!* Indeed, for $\frac{\pi^2}{2} < \gamma < \gamma_* \approx 11.561$, the function F *does have* a ladder of resonances, but as we shall show in the next section, it *has no* real zeroes. So, our ladder of resonances or eigenvalues exists due to some other reasons and the existence of the zero-width resonances is mostly the implication of the presence of such ladder and its behavior as γ varies.

5 Spectral singularities

5.1 General analytical expressions

In this section we study real zeroes of the function F corresponding to spectral singularities, i.e. to zero-width resonances. For such zeroes, equation (2.9) is a pair of two real equations for one real variable k and two parameters ℓ and γ . Thanks to the symmetry of the zeroes with respect to the imaginary axis, it is sufficient to find only positive real resonances since the negative ones are located symmetrically with respect to the origin. Similar to the proof of Lemma 5, for real positive k we make change (3.17)

and rewrite equation (2.9) in the following form:

$$(1 - 2u^{-4}) \cos \beta u^{-1} + (2u^4 - 1) \cosh \beta u + 2i\sqrt{1 - u^4} (u^2 \sinh \beta u - u^{-4} \sin \beta u^{-1}) - e^{-2i\beta\ell\sqrt{u^{-2} - u^2}} (\cosh(\beta u) - \cos \beta u^{-1}) = 0, \quad \beta = \sqrt{2}\gamma.$$

Taking the real and imaginary part of this equation and multiplying the equation by u^4 , we obtain:

$$\begin{aligned} (u^4 - 2) \cos \beta u^{-1} + u^4(2u^4 - 1) \cosh \beta u &= u^4 \cos \left(2\beta\ell\sqrt{u^{-2} - u^2} \right) (\cosh \beta u - \cos \beta u^{-1}), \\ 2\sqrt{1 - u^4} (u^6 \sinh \beta u - \sin \beta u^{-1}) &= -u^4 \sin \left(2\beta\ell\sqrt{u^{-2} - u^2} \right) (\cosh \beta u - \cos \beta u^{-1}). \end{aligned} \quad (5.1)$$

This is a system of two real equations with three real variables. If we are given (β, ℓ) and we try to find u , the system is overdetermined and does not necessary have a root. In other words, it is solvable with respect to u only if (β, ℓ) are located on some (solvability) curves. In order to avoid working with an overdetermined system, in what follows we regard (5.1) as a system for two unknown variable with one parameter.

To find the curves in (β, ℓ) plane, on which equations (5.1) are solvable with respect to u , we shall regard u as a parameter and (β, ℓ) as unknown variables. We take the sum of squares of equations (5.1) and divide the result by $(1 - u^4)$. We also divide equations (5.1). This leads us to a pair of equations:

$$\begin{aligned} u^4(1 - u^4) \cosh \beta u \cos \beta u^{-1} - 2u^6 \sinh \beta u \sin \beta u^{-1} + 1 - u^{12} &= 0, \\ \frac{2\sqrt{1 - u^4}(u^6 \sinh \beta u - \sin \beta u^{-1})}{(2 - u^4) \cos \beta u^{-1} + u^4(1 - 2u^4) \cosh \beta u} &= \tan \left(2\beta\ell\sqrt{u^{-2} - u^2} \right). \end{aligned} \quad (5.2)$$

The second equation can be solved explicitly with respect to ℓ :

$$\ell = \frac{1}{2\beta\sqrt{u^{-2} - u^2}} \left(\arctan \frac{2\sqrt{1 - u^4}(u^6 \sinh \beta u - \sin \beta u^{-1})}{(2 - u^4) \cos \beta u^{-1} + u^4(1 - 2u^4) \cosh \beta u} + \pi n \right), \quad (5.3)$$

where $n \in \mathbb{N}$ is an arbitrary natural number. As the next lemma states, to make equations (5.2), (5.3) equivalent to (5.1), we should also assume that

$$(-1)^n = \text{sign}((u^4 - 2) \cos \beta u^{-1} + u^4(2u^4 - 1) \cosh \beta u). \quad (5.4)$$

Lemma 8. *Equations (5.1) are equivalent to (5.2), (5.3), (5.4).*

Proof. We rewrite shortly equations (5.1) as $A_1 = B \cos \alpha$, $A_2 = -B \sin \alpha$, where A_1, A_2 are the left hand sides in (5.1), $\alpha = 2\beta\ell\sqrt{u^{-2} - u^2}$ and $B = u^4(\cosh \beta u - \cos \beta u^{-1})$. Then equations (5.2), (5.3) become $A_1^2 + A_2^2 = B^2$, $\alpha = -\arctan \frac{A_2}{A_1} + \pi n$. We have:

$$B \cos \alpha = (-1)^n \cos \arctan \frac{A_2}{A_1} = \frac{(-1)^n}{\sqrt{1 + \frac{A_2^2}{A_1^2}}} = \frac{(-1)^n |A_1|}{\sqrt{A_1^2 + A_2^2}}$$

and we get the first equation $A_1 = B \cos \alpha$ provided condition (5.4) is satisfied. In the same way we check that the latter condition also ensures the second equation $A_2 = -B \sin \alpha$. \square

Equation (5.2) is transcendental, and we can not solve it analytically. Nevertheless, for each $u \in (0, 1)$, this is an equation only for a single variable β , not for two as equations (5.1). So, we propose the following algorithm of recovering the aforementioned solvability curves: choose $u \in (0, 1)$, then solve equation (5.2) and recover the sequence of distances ℓ by formula (5.3) with different integer n . Then the gain-and-loss amplitude γ and the corresponding wavenumber k can be readily recovered from β and u . In a similar way, one can first fix some value of β (i.e., fix the gain-and-loss strength) and then

solve equation (5.2) with respect to u and recover ℓ by (5.3). Equation (5.2) is well-behaved, and for each β all its zeros u can be easily found numerically.

Alternatively, as explained below in Section 5.5, the values corresponding to spectral singularities can be found systematically by means of the numerical continuation from the limit $\ell = 0$. However, in this case equation (5.2) is still useful because it allows one to check that all spectral singularities have been found for the given value of the gain-and-loss γ .

5.2 Absence of spectral singularities

For $u = 0$ and $u = 1$, the left-hand-side of equation (5.2) is equal respectively to 1 and $-2 \sinh \beta \sin \beta$. Then a sufficient condition for the existence of a spectral singularity at the given gain-and-loss amplitude γ is $\sin \beta = \sin \sqrt{2\gamma} > 0$. At the same time, it is also possible to establish sufficient conditions that forbid the existence of spectral singularities in a certain interval of parameters. In this subsection we prove the existence of two “forbidden gaps” for the roots of equation (5.2). The first one exists for all $\beta \geq 0$ and it states that there is no roots in certain interval. The second gap is a certain interval of values of β , for which equation (5.2) has no zeroes at all.

For the convenience, by $g(u, \beta)$ we denote the left hand side of equation (5.2). The first “forbidden gap” is described in the following lemma.

Lemma 9. *For all $\beta \geq 0$, equation (5.2) has no roots in the interval $[0, (1 + \frac{\beta}{4})^{-1}]$.*

Proof. Employing a standard inequality $a \cos \alpha + b \sin \alpha \leq \sqrt{a^2 + b^2}$, we estimate the first two term in equation (5.2) as

$$u^4(1 - u^4) \cosh \beta u \cos \beta u^{-1} - 2u^6 \sinh \beta u \sin \beta u^{-1} \leq \sqrt{u^8(1 - u^4)^2 \cosh^2 \beta u + 4u^{12} \sinh^2 \beta u}.$$

Hence, equation (5.2) surely has no roots for values of u satisfying

$$\sqrt{u^8(1 - u^4)^2 \cosh^2 \beta u + 4u^{12} \sinh^2 \beta u} < 1 - u^{12}.$$

Expressing $\cosh^2 \beta u$ via $\sinh^2 \beta u$ and simplifying this inequality, we obtain $u^4(1 + u^4) \cosh \beta u < 1 + u^{12}$ and hence,

$$\cosh \beta u - 1 < \frac{1 - 2u^4 + u^8}{u^4}, \quad \sqrt{2} \sinh \beta u < u^{-2} - u^2. \quad (5.5)$$

Thanks to the estimate $\sqrt{2} \sinh 2 \ln u^{-1} \leq u^{-2} - u^2$, $u \in (0, 1]$, the last inequality in (5.5) holds once $\frac{\beta}{4} < u^{-1} \ln u^{-1}$. It is easy to confirm that this inequality is true once $u^{-1} > 1 + \frac{\beta}{4}$. The proof is complete. \square

The next lemma is auxiliary and will be employed in studying the second forbidden zone.

Lemma 10. *The function $g(u, \pi)$ is positive on $[0, 1)$.*

Proof. We have $g(0, \pi) = 1$ and by Lemma 9, it is positive for $u < (1 + \frac{\pi}{4})^{-1}$. This is why in what follows we consider only the values $u \geq (1 + \frac{\pi}{4})^{-1}$. For such values of u we have $\pi \leq \pi u^{-1} \leq \pi(1 + \frac{\pi}{4}) < 1.79\pi$. As $\frac{3\pi}{2} \leq \pi u^{-1} \leq \pi(1 + \frac{\pi}{4})$, the function $\sin \beta u^{-1}$ is negative, while $\cos \beta u^{-1}$ is positive. Hence, for such values of u , the function $g(u, \pi)$ is positive. It remains to consider the values $\frac{2}{3} < u \leq 1$.

For such values of u we first observe the following simple estimates:

$$\frac{1 - u^4}{1 - u} \cos \pi u^{-1} \geq -4, \quad -\frac{\sin \pi u^{-1}}{1 - u} = \frac{\sin \pi(u^{-1} - 1)}{1 - u} \geq \pi u.$$

Then the function g satisfies the estimate:

$$\frac{g(u, \pi)}{u^4(1 - u)} \geq g_1(u) + g_2(u), \quad g_1(u) := -4 \cosh \pi u + 2\pi u^3 \sinh \pi u, \quad g_2(u) := \frac{1 - u^{12}}{u^4(1 - u)}. \quad (5.6)$$

The function $g_1(u)$ is monotonically increasing in $u \in [\frac{2}{3}, 1]$ since

$$g_1'(u) = 2\pi^2 u^3 \cosh \pi u + (6\pi u^2 - 4\pi) \sinh \pi u > 2\pi(\pi u^3 + 6u^2 - 2) \sinh \pi u > 2\pi \sinh \pi u > 0.$$

Hence, $g_1(u) \geq g_1(\frac{2}{3}) > -9.05$. For the function g_2 we have the following representation and estimate:

$$g_2(u) = 1 + \sum_{j=1}^4 (u^j + u^{-j}) + \sum_{j=5}^8 u^j \geq 9 + \sum_{j=5}^8 \left(\frac{2}{3}\right)^j > 9.31.$$

Two last estimates and (5.6) imply the positivity of the function g for $u \in [\frac{2}{3}, 1]$. \square

Denote

$$g_*(u, \beta) := \beta u^3(1 - 3u^4) \cosh \beta u \sin \beta u^{-1} + \beta u^5(3 - u^4) \sinh \beta u \cos \beta u^{-1} - 2u^4(1 + u^4) \cosh \beta u \cos \beta u^{-1} - 6(1 + u^{12}).$$

The next lemma states the existence of the second forbidden zone.

Lemma 11. *Equation (5.2) has no roots as $\pi < \beta < \beta_*$, where (u_*, β_*) is the root of the system of the equations*

$$g(u, \beta) = 0, \quad g_*(u, \beta) = 0, \quad u \in [0, 1], \quad \pi < \beta < 5, \quad (5.7)$$

with minimal possible β . Their approximate values are

$$\beta_* = 4.808438, \quad u_* = 0.611772. \quad (5.8)$$

Proof. The function $g(u, \pi)$ is positive on $[0, 1)$ and $g(1, \pi) = 0$, see Figure 3a. As $\pi < \beta < 2\pi$, we have $g(0, \beta) = 1 > 0$ and $g(1, \beta) = -2 \sin \beta \sinh \beta > 0$. Hence, for β close enough to π , the function $g(u, \beta)$ is positive for all $u \in [0, 1]$. At the same time, we have $g(0.65, 5) < -0.617 < 0$ and therefore, for $\beta = 5$, equation (5.2) possesses at least two roots, one in $(0, 0.65)$ and another in $(0.65, 1)$. cf. Figure 3c. We also observe that the function g is jointly continuous in (u, β) . The above facts means that as β grows from π to 5, at some value $\beta = \beta_*$, the graph of the function g is still located in the upper half-plane but touches the u -axis at some point $u = u_*$, see Figure 3b. The function $g(u, \beta)$ is positive as $\pi < \beta < \beta_*$ and $u \in [0, 1]$. Then the point $u = u_*$ is obviously the global minimum of g and hence, (u_*, β_*) is a solution to the system of equations $g(u, \beta) = 0$, $\frac{\partial g}{\partial u}(u, \beta) = 0$. It is easy to check that $g_* = \frac{\partial g}{\partial u} - 6g$ and hence, (u_*, β_*) solves system (5.7). These roots can be found numerically and this gives (5.8). The proof is complete. \square

Returning from the auxiliary variable β to the gain-and-loss amplitude $\gamma = \beta^2/2$, from Lemma 11 we deduce the following important result:

$$\text{there is no spectral singularities for } \frac{\pi^2}{2} < \gamma < \gamma_* \approx 11.561. \quad (5.9)$$

5.3 Creating a spectral singularity at a given wavenumber

For $\ell = 0$ spectral singularity can only be obtained for some isolated values of the wavenumber k and the gain-and-loss amplitude γ [1]. Several lowest values of γ corresponding to the spectral singularities and the associated wavenumbers k are listed in Table 1. An important advantage of the more general system with nonzero gain-to-loss distance $\ell > 0$ consists in the possibility to create a spectral singularity at any wavenumber k given beforehand. Indeed, let us return back to equations (5.2), (5.3) and discuss the following issue: given a point k on the real axis, how to choose β and ℓ to have a resonance at this point? Equations (5.2)–(5.3) allow us to answer easily this question.

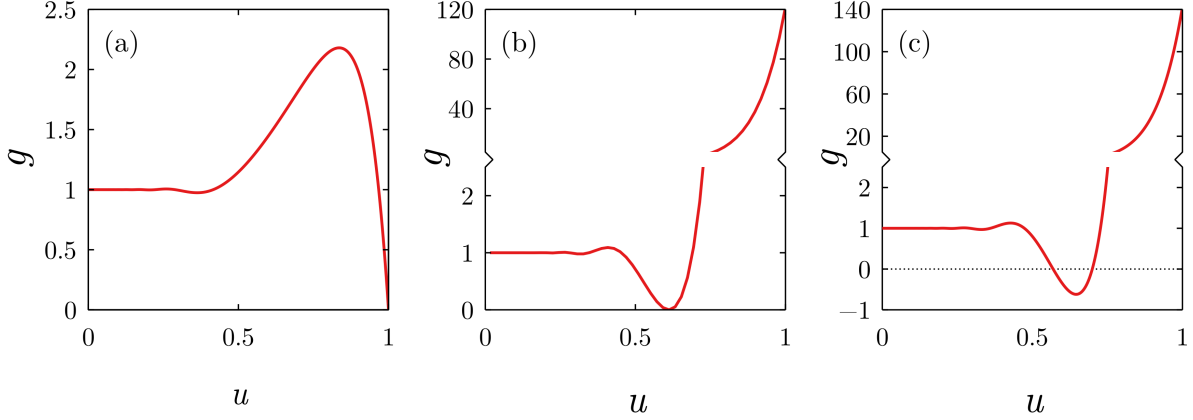


Figure 3: Illustration for proof of Lemma 11. Graphs of the function $g(u, \beta)$ for $\beta = \pi$ (a), $\beta = \beta_* \approx 4.808438$ (b), and $\beta = 5$ (c). Notice broken vertical axes in (b) and (c).

n	0	1	2
$\gamma_*^{(n)}$	2.071	13.307	27.783
$k_*^{(n)}$	1.065	4.318	7.529

Table 1: Approximate values of gain-and-loss amplitudes $\gamma = \gamma_*^{(n)}$ and wavenumbers $k = k_*^{(n)}$, $n = 0, 1, \dots$, corresponding to spectral singularities with lowest γ in the limit $\ell = 0$, see Table I in [1].

We fix $k > 0$ and we find the associated value of u by resolving (3.17):

$$u^{-2} - u^2 = 4k^2\beta^{-2}, \quad u = \beta R^{-1}, \quad \text{where } R = \sqrt{2k^2 + \sqrt{4k^4 + \beta^4}}. \quad (5.10)$$

We divide equation (5.2) by u^6 and substitute then the above formulae and

$$\frac{1 - u^{12}}{u^6} = \frac{1 - u^4}{u^2} \frac{1 + u^4 + u^8}{u^4} = (u^{-2} - u^2)((u^{-2} - u^2)^2 + 3).$$

This gives the equation:

$$2\beta^4 k^2 \cosh(\beta^2 R^{-1}) \cos R - \beta^6 \sinh(\beta^2 R^{-1}) \sin R + 2k^2(16k^4 + 3\beta^4) = 0. \quad (5.11)$$

An algorithm for creating a resonance at a prescribed point k is as follows. Given $k > 0$, we first solve equation (5.11) with respect to β and we also find u by (5.10). Then needed values of ℓ are determined by (5.3), (5.4).

In order to illustrate this algorithm, we consider a finite interval of wavenumbers $k \in (0, k_1]$, where we set $k_1 = 10$ for the numerics reported on in what follows. We scan the chosen interval with a sufficiently small step ($\Delta k = 0.01$) and for each value of k solve equation (5.11) numerically using the simple dichotomy method. While for each k equation (5.11) might have several roots β , in our numerical procedure we always choose the minimal positive root, i.e., the one which allows to achieve the spectral singularity with given k at the smallest possible value of the gain-and-loss amplitude $\gamma = \gamma_{\min}$. Next, we choose the minimal positive distance ℓ_{\min} which satisfies the conditions (5.3), (5.4) and then we use the periodicity in ℓ to generate the sequence of larger gain-to-loss distances $\ell_n = \ell_{\min} + n\pi/(2k)$, $n = 1, 2, \dots$ [see (3.2)]. The resulting dependencies $\gamma_{\min}(k)$ and $\ell_{\min}(k)$, $\ell_n(k)$ are shown in figure 4. The minimal gain-and-loss amplitude $\gamma_{\min}(k)$ and the minimal gain-to-loss distance ℓ_{\min} are discontinuous, which means that the small variation in the wavenumber k might require a significant change either in

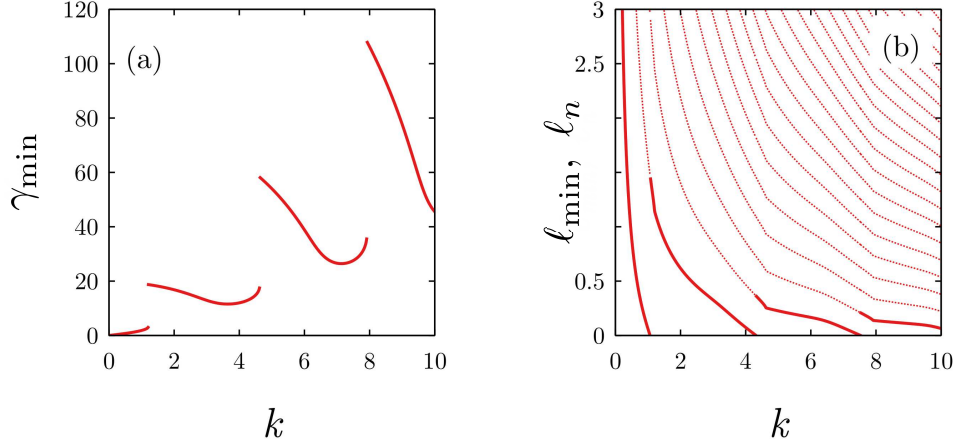


Figure 4: (a) Minimal value of the gain-and-loss amplitude γ_{\min} which corresponds to a spectral singularity with the given value of the wavenumber k . (b) Minimal gain-to-loss distance ℓ_{\min} which corresponds to a spectral singularity with the k and γ from the left panel (bold curves) and larger distances ℓ_n obtained using the periodicity in ℓ (thin dotted curves).

γ or in ℓ . It is especially important that the values of the distance ℓ are generically different from zero, which points out explicitly that the new degree of freedom offered by the nonzero gain-to-loss distance is important for the achieving a spectral singularity at the given wavenumber k .

5.4 \mathcal{PT} -symmetry breaking laser-antilaser threshold

A particularly important characteristics of any \mathcal{PT} -symmetric structure is the \mathcal{PT} symmetry breaking threshold, i.e., the amplitude of the gain-and-loss corresponding to the “phase transition” from the purely real to complex spectrum. The best studied scenario of the phase transition is the collision of two real discrete eigenvalues at an exceptional point with the subsequent splitting in a complex-conjugate pair. However, in systems with nonempty continuous spectrum, the phase transition can also occur through the splitting of a self-dual spectral singularity, which results in a bifurcation of a complex-conjugate pair from an interior point of the continuum [44, 45, 47]. At the moment corresponding to the formation of the spectral singularity, the system operates in the CPA-laser regime [2]. Thus, in such a system, the \mathcal{PT} -symmetry breaking threshold at the same time corresponds to the CPA-laser threshold.

Lemma 3 guarantees that the spectrum of our system is real for sufficiently small gain-and-loss amplitudes γ . Additionally, according to Lemma 7, the spectrum does not have any real discrete eigenvalue. Hence, the \mathcal{PT} -symmetry breaking is expected to occur through the emergence of a self-dual spectral singularity. In order to identify the \mathcal{PT} -symmetry breaking threshold in our system, we start from the limit $\ell = 0$, there the phase transition takes place at $\gamma_{\star}^{(0)} \approx 2.072$, see [1, 45] and Table 1. Thus, the spectrum with $\ell = 0$ is purely real and continuous for $\gamma \in [0, \gamma_{\star}]$, while the increase of the gain-and-loss just above $\gamma_{\star}^{(0)}$ leads to the bifurcation of a complex-conjugate pair from an interior point of the continuum. The spectral singularity forming at $\gamma_{\star}^{(0)}$ takes place at wavenumber $k = k_{\star}^{(0)} \approx 1.065$. Respectively, the complex-conjugate pair of eigenvalues bifurcates from $\lambda_0 = [k_{\star}^{(0)}]^2$. (Notice that the further increase of γ above the next threshold values listed in Table 1 leads to the formation of new spectral singularities and, respectively, to bifurcations of new complex-conjugate pairs in the spectrum.)

Next, we use the numerical continuation in ℓ in order to continue the known solution at $\ell = 0$ to the domain $\ell > 0$. The obtained dependence of the threshold value of the gain-and-loss amplitude on distance ℓ is shown in figure 5(a), where we observe that the phase transition threshold decreases monotonically with the growth of ℓ . This means that introducing an additional space between the

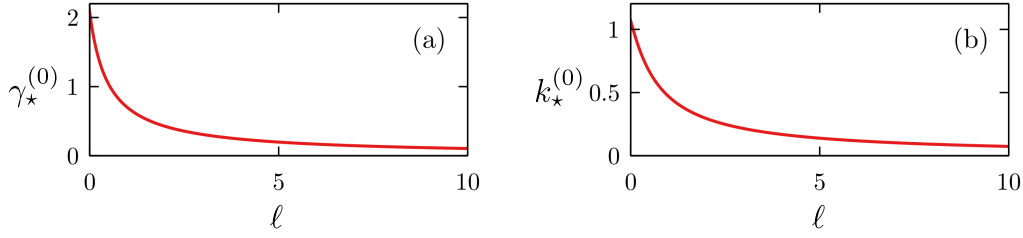


Figure 5: (a) \mathcal{PT} -symmetry breaking threshold $\gamma_\star^{(0)}$ vs the distance between the gain and loss ℓ . The spectrum is purely real and continuous for $\gamma \leq \gamma_\star$, but acquires a pair of complex conjugate eigenvalues as the gain-and-loss amplitude exceeds the threshold $\gamma_\star^{(0)}$. (b) Values of the wavevector $k_\star^{(0)}$ corresponding to the dependence in (a).

gain and loss, one can decrease the \mathcal{PT} -symmetry breaking threshold, i.e. achieve the laser-antilaser operation at lower gain-and-loss amplitudes than in a waveguide with the adjacent gain and loss.

5.5 General picture of spectral singularities

Let us now turn to description of the general picture of spectral singularities. In order to construct systematically different solutions, we again start from the limit $\ell = 0$, where the values of γ and k corresponding to spectral singularities are known, see Table 1. Then we use the periodicity of function $e^{-4ik\ell}$ in ℓ in order to construct new branches of solutions having no counterparts in the limit $\ell = 0$, cf. equation (3.2). This procedure results in a fairly complicated picture containing a multitude of spectral singularities, some part of which (corresponding to relatively small values of the gain-and-loss) is shown in figure 6(a,b) as the curves on the plane γ vs ℓ and k vs ℓ .

Let us describe the structure of the found solutions using the diagram γ vs ℓ in figure 6(a). The multitude of curves shown in this plot can be divided into three groups (plotted with red, blue and green curves) which have been obtained by means of the continuation from three different solutions in the limit $\ell = 0$. There is a well-visible vertical gap between red and blue curves, which corresponds to the “forbidden” values of the gain-and-loss amplitudes γ found above in (5.9). At the same time, there is no gap between blue and green curves, which results in a multitude of intersections between these curves. The first group of spectral singularities, corresponding to red curves in Figure 6(a), is obtained through the continuation from the spectral singularity in the limit $\ell = 0$ with the smallest gain-and-loss amplitude, i.e. from values $\gamma_\star^{(0)}$ and $k_\star^{(0)}$ in Table 1. The leftmost (bold) curve in this group which originates in the limit $\ell = 0$ is the \mathcal{PT} -symmetry breaking threshold which was already shown in figure 5(a). For values of γ above this curve, there is always one or more (but finitely many, see Section 4) complex-conjugate pairs of eigenvalues in the spectrum. Several curves situated to the right from the bold red curve are obtained using the fact that if γ and k are solutions in the limit $\ell = 0$, then the same values of γ and k also correspond to a spectral singularity with $\ell_n = (n\pi)/(2k)$, $n = 1, 2, \dots$. Once a single solution with a new distance ℓ_n is obtained, a new branch of solutions can be constructed using numerical continuation in γ or in ℓ . In the limit $\ell \rightarrow \infty$ all the red curves in figure 6(a) approach the asymptotic value $\gamma = 0$ or at $\gamma_\star = \pi^2/2 \approx 4.935$. Notice that, except for the bold line demarcating the \mathcal{PT} -symmetry breaking threshold, none of the red curves can be continued to the limit $\ell \rightarrow 0$.

The multitude of red curves in figure 6(a) demonstrates explicitly how new spectral singularities emerge with the increase of ℓ . Indeed, drawing an imaginary horizontal line, say, at $\gamma = 3$ [see the vertical axis tick in figure 6(a)], we observe that with the increase of ℓ this line intersects more and more red curves. Each intersection corresponds to the values of γ and ℓ at which some root k crosses the real axis and goes down from the upper to lower complex half-plane. Thus, a finite-width resonance transforms to a complex eigenvalue through the spectral singularity (we recall again that in view of \mathcal{PT} symmetry any root $k \neq 0$ crosses the real line simultaneously with its counterpart $-\bar{k}$, i.e. the

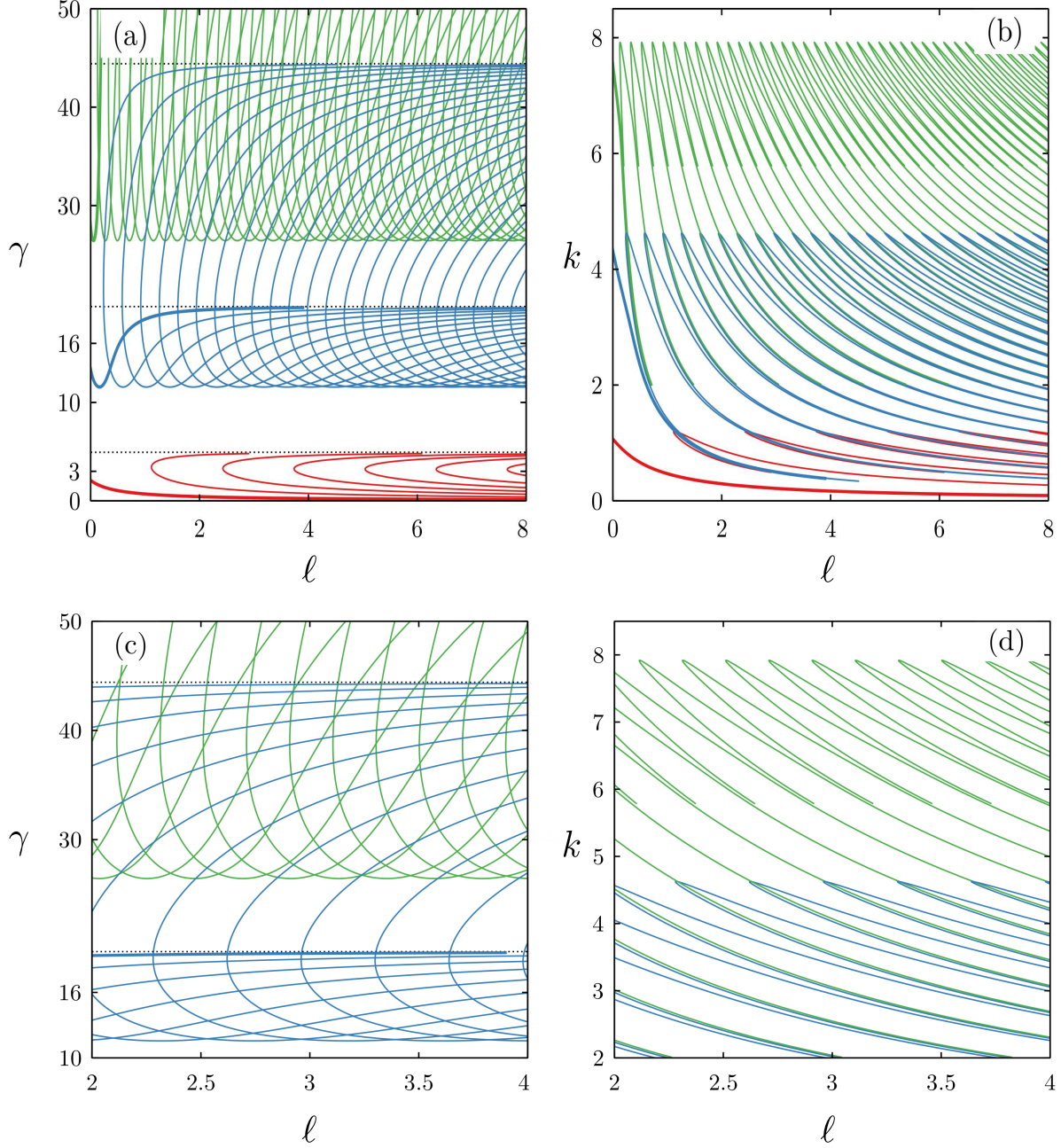


Figure 6: (a) Values of the gain-and-loss amplitude γ and distance ℓ , for which spectral singularities occur. (b) Corresponding wavenumbers k . Panel (c) magnifies the region $(\ell, \gamma) \in [2, 4] \times [10, 50]$ from (a), and panel (d) is the magnification of corresponding curves from panel (b).

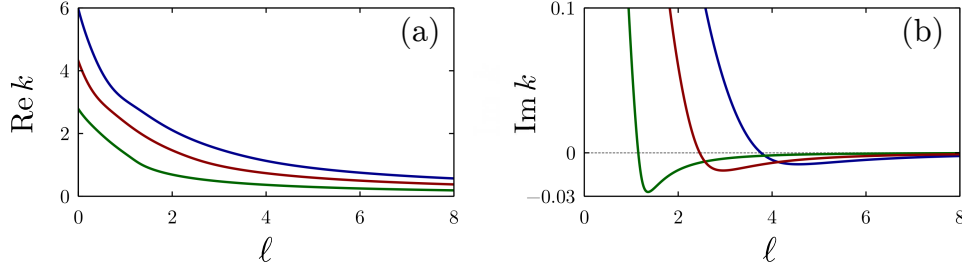


Figure 7: (a,b) Real and imaginary parts of three complex zeros of function F for fixed $\gamma = 3$ and increasing ℓ . For each curve, the imaginary part is positive for small ℓ and becomes negative for all sufficiently large ℓ . For each three shown eigenvalues, its real and imaginary parts are of the same colour in both panels.

corresponding spectral singularity is self-dual). In order to illustrate this process, in Figure 7 we show the evolution of three numerically found complex zeros of function $F(k, \gamma, \ell)$ under the increase of ℓ . In this figure the imaginary part of each complex zero changes sign from positive to negative and then asymptotically approaches zero (remaining negative). In the limit of large ℓ , this behavior agrees with expansion (3.10) of Lemma 4, where, for the chosen value of γ , we have $\sin \sqrt{2\gamma} > 0$. Thus the growing distance ℓ results in a sequence of self-dual spectral singularities and in the increasing number of complex-conjugate eigenvalues in the spectrum.

The second group of spectral singularities [blue curves in figure 6(a)] was obtained by means of the continuation from the next solution in the limit $\ell = 0$, i.e. from $\gamma_\star^{(1)}$ and $k_\star^{(1)}$ in Table 1. Again, one of the curves [the leftmost bold curve in figure 6(a)] was obtained through the direct continuation from the limit $\ell = 0$, while other blue curves were generated using the periodicity of function $F(k, \gamma, \ell)$ in ℓ and cannot be continued to the limit $\ell \rightarrow 0$. In the limit $\ell \rightarrow \infty$ the blue curves approach the horizontal asymptotes $\gamma = 2\pi^2 \approx 19.739$ and $\gamma = 9\pi^2/2 \approx 44.413$. In the (γ, ℓ) -plane the gain-and-loss amplitudes corresponding to the group of blue curves are well separated from those for the red curves: indeed, all red curves are bounded from above by the asymptote $\gamma = \pi^2/2 \approx 4.935$, while all blue curves are bounded from below by $\gamma_\star \approx 11.561$, see (5.9). Thus, the emergence of new spectral singularities with the increase of ℓ is sensitive to the value of the gain-and-loss amplitude and does not occur for the gain-and-loss amplitudes lying in the gap between the red and blue curves.

In comparison with the red curves discussed above, the curves from the blue group in figure 6(a) feature more complicated behavior and, in particular, can intersect each other (and also intersect the curves from the next, third group of green curves discussed below). The intersections between the blue curves occur for the gain-and-loss amplitudes in the interval $11.561 \lesssim \gamma < 9\pi^2/2 \approx 19.739$, where $\sin \sqrt{2\gamma}$ is negative. At first glance, this might seem to contradict to the expansion (3.10) of Lemma 4, which suggests that in this case the multitude of complex zeros accumulate in the upper complex half-plane with the growth of ℓ . However, this apparent contradiction is resolved if we trace the behavior of the complex roots more closely. Indeed, choosing for an example $\gamma = 16$ [see the vertical axis tick in figure 6(a)] and computing several complex roots under the increase of ℓ , we observe that each considered root first goes down from the upper half-plane to the lower one but then again returns to the upper half-plane, see Figure 8(b) and (b₁). Thus, in this interval of the gain-and-loss amplitudes the increase of ℓ results either in the transformation from the resonance to the eigenvalue or to the opposite process, i.e. to the disappearance of the complex-conjugate pair. Respectively, the intersection between the two blue curves corresponds to two coexisting spectral singularities, i.e. to the moment when one complex-conjugate pair of eigenvalues disappears and another pair (with different k) emerges. For sufficiently large ℓ the imaginary part of each considered root remains positive and approaches zero, in accordance with expansion (3.10). Thus, in this interval of the gain-and-loss strengths, the limit $\ell \rightarrow \infty$ the spectrum contains only a finite number of complex-conjugate eigenvalues, which correspond

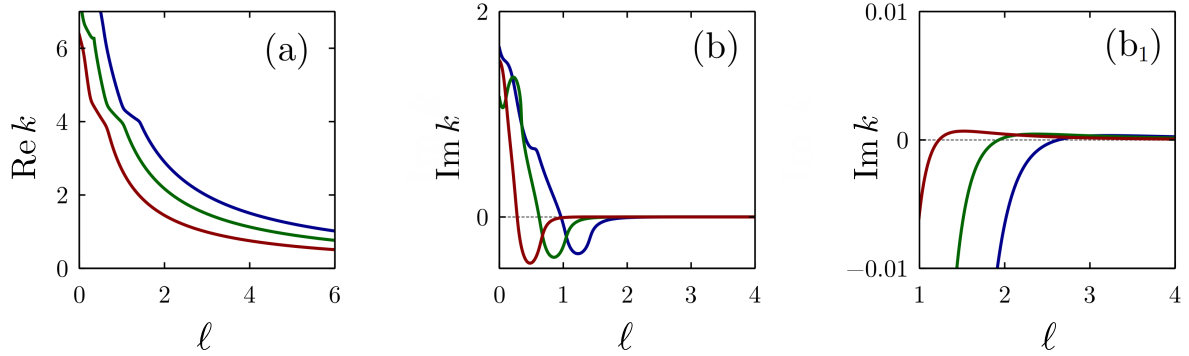


Figure 8: (a,b) Real and imaginary parts for three complex zeros of function F for fixed $\gamma = 16$ and increasing ℓ . Panel b_1 is the magnification of some region of (b) and shows more clearly that imaginary parts of all three shown eigenvalues are positive for all sufficiently large ℓ . For each three shown eigenvalues, its real and imaginary parts are of the same colour in both panels.

to complex zeros k whose behavior is not covered by expansion (3.10).

The third group of spectral singularities [green curves in figure 6(a)] was obtained by means of the continuation from the solution $\gamma_\star^{(2)}$ and $k_\star^{(2)}$ in Table 1. In view of the very complicated structure of the overall resulting picture, we only show a section of these curves corresponding to relatively small values of the gain-and-loss amplitudes γ . Quite interestingly, there is no gap between the blue and green groups of curves, which results in the multitude of intersections between blue and green curves, see Fig. 6(a) and the magnified view in Fig. 6(c). These intersections suggest a possibility of simultaneous emergence of two complex-conjugate pairs of eigenvalues from two different interior points of the continuous spectra.

Considering further solutions $\gamma_\star^{(n)}$, $k_\star^{(n)}$, $n = 3, 4, \dots$, in the limit $\ell = 0$ one can construct new groups of spectral singularities with larger values of γ , which are not shown in Figure 6.

6 Conclusion

A pair of geometrically identical absorptive and active elements is the simplest realization of a \mathcal{PT} -symmetric system. Properties of \mathcal{PT} -symmetric systems are usually considered subject to the change of the gain-and-loss amplitude. In the present work, we have approached the problem from a different perspective and considered how the spectral properties of the \mathcal{PT} -symmetric waveguide depends on the distance between gain and loss elements. We have derived a compact equation for resonances, spectral singularities and bound states and analyzed it in detail for different gain-to-loss distances.

The first main result of our study shows that in the limit of large gain-to-loss distances the \mathcal{PT} -symmetric waveguide feature a ladder of resonances, which resembles the well-known Wannier-Stark ladder for periodic lattices with an additional linear potential. The number of resonances increases as the gain-to-loss distance grows. Moreover, changing the gain-and-loss amplitude, one can transform a ladder of resonances to a ladder of complex-conjugate eigenvalues — the feature which is not accessible in Hermitian (self-adjoint) systems.

The transformation from a resonance to an eigenvalue corresponds to a self-dual spectral singularity, i.e. to a zero-width resonance in the continuous spectrum. Transition through a self-dual spectral singularity corresponds to a bifurcation of a complex-conjugate pair of eigenvalues from an interior point of the continuous spectrum. Our second main result consists in the detailed study of spectral singularities that emerge in the system with varying gain-to-loss distance. We have demonstrated that by choosing a proper distance between the gain and loss, one can achieve a spectral singularity at any wavenumber (which is not possible in the waveguide with adjacent gain and losses, where spectral singularities occur only at certain isolated values of the wavenumber). We have also demonstrated

that the increase of the distance between gain and loss reduces the \mathcal{PT} -symmetry breaking threshold and, respectively, allows to achieve coherent perfect absorption-laser operation (alias, laser-antilaser regime) at a lower value of the gain-and-loss amplitude. Using the fact that the equation determining the spectral singularities is periodic in the gain-to-loss distance ℓ , we have demonstrated how one can generate systematically spectral singularities at subsequently increasing distances. In particular, it is possible to generate the branches of spectral singularities that do not have a counterpart in the limit $\ell = 0$. By tuning the gain-and-loss amplitude and a distance, one can reach a situation when two different self-dual spectral singularities emerge *simultaneously* (but, generically speaking, with different wavenumbers). This suggests that two pairs of complex-conjugate eigenvalues can emerge from two different interior points of the continuous spectrum simultaneously. Additionally, this observation defies conjecture (ii) in Conclusion of [46] where it is suggested that a parametrically fixed \mathcal{PT} -symmetric complex potential has at most one spectral singularity. Thus, in spite of its apparent simplicity, the \mathcal{PT} -symmetric model with spaced gain and loss elements essentially enriches the previously known phenomenology.

Acknowledgments

The results concerning the large distance regime (Lemmata 4, 5, 6 and Section 4.2) were financially supported by Russian Science Foundation (project No. 17-11-01004). The results by D.A.Z. on spectral singularities were obtained with the support from Russian Foundation for Basic Research, project No. 19-02-00193\19.

References

- [1] Mostafazadeh A 2009 Spectral singularities of complex scattering potentials and infinite reflection and transmission coefficients at real energies *Phys. Rev. Lett.* **102** 220402
- [2] Longhi S 2010 \mathcal{PT} -symmetric laser absorber *Phys. Rev. A* **82** 031801(R)
- [3] Peng B, Özdemir Ş K, Lei F, Monifi F, Gianfreda M, Long G, Fan S, Nori F, Bender C M and Yang L 2014 Loss-induced suppression and revival of lasing *Nat. Phys.* **10** 394
- [4] Lin Z, Ramezani H, Eichelkraut T, Kottos T, Cao H, and Christodoulides D N 2011 Unidirectional invisibility induced by \mathcal{PT} -symmetric periodic structures *Phys. Rev. Lett.* **106** 213901
- [5] Bender C M, Berntson B K, Parker D and Samuel E 2013 Observation of PT phase transition in a simple mechanical system *Am. J. Phys.* **81** 173-179
- [6] Ruschhaupt A, Delgado F and Muga J G 2005 Physical realization of \mathcal{PT} -symmetric potential scattering in a planar slab waveguide *J. Phys. A: Math. Gen.* **38** L171-L176
- [7] El-Ganainy R, Makris K G, Christodoulides D N and Musslimani Z H 2007 Theory of coupled optical \mathcal{PT} -symmetric structures *Opt. Lett.* **32** 2632-2634
- [8] Rüter C E, Makris K G, El-Ganainy R, Christodoulides D N, Segev M and Kip D 2010 Observation of parity-time symmetry in optics *Nat. Phys.* **6** 192-195
- [9] Zyablovsky A A, Vinogradov A P, Pukhov A A, Dorofeenko A V and Lisiansky A A 2014 PT-symmetry in optics *Physics – Uspekhi* **57** 1063–1082
- [10] Konotop V V, Yang J and Zezyulin D A 2016 Nonlinear waves in \mathcal{PT} -symmetric systems *Rev. Mod. Phys.* **88** 035002

- [11] Longhi S 2017 Parity-time symmetry meets photonics: A new twist in non-Hermitian optics *EPL* **120** 64001
- [12] Feng L, El-Ganainy R, and Ge L 2017 Non-Hermitian photonics based on paritytime symmetry *Nat. Photonics* **11** 752762
- [13] El-Ganainy R, Makris K G, Khajavikhan M, Musslimani Z H, Rotter S. and Christodoulides D N 2018 Non-Hermitian physics and PT symmetry *Nat. Phys.* **14** 11-19
- [14] Gluck M, Kolovsky A R and Korsch H J 2002 Wannier-Stark resonances in optical and semiconductor superlattices *Phys. Rep.* **366** 103182
- [15] Davies E B 1982 The twisting trick for double well Hamiltonians *Comm. Math. Phys.* **85** 471–479
- [16] Aventini P and Seiler R 1975 On the electronic spectrum of the diatomic molecular ion *Comm. Math. Phys.* **41** 119–134
- [17] Harrell E M 1980 Double wells *Comm. Math. Phys.* **75** 239–261
- [18] Morgan III J D and Simon B 1980 Behavior of molecular potential energy curves for large nuclear separations *Int. J. Quantum Chem.* **17** 1143–1166
- [19] Klaus M and Simon B 1979 Binding of Schrödinger particles through conspiracy of potential wells *Ann. Ins. Henri Poincaré section A* **30** 83–87
- [20] Graffi V, Harrell II E M and Silverstone H J 1985 The $\frac{1}{R}$ expansion for H_2^+ : analyticity, summability and asymptotics *Ann. Phys.* **165** 441–483
- [21] Borisov D and Golovina A 2012 On the resolvents of periodic operators with distant perturbations *Ufa Math. J.* **4** 65–73
- [22] Borisov D, Exner P and Golovina A 2012 Tunneling resonances in systems without a classical trapping *J. Math. Phys.* **54** 012102
- [23] Golovina A M 2012 On the resolvent of elliptic operators with distant perturbations of whole space *Russ. J. Math. Phys.* **19** 182–192
- [24] Golovina A M 2014 On the spectrum of elliptic operators with distant perturbation in the space *St. Petersburg Math. J.* **25** 735–754
- [25] Klopp F and Fedotov A A 2016 Stark–Wannier ladders and cubic exponential sums *Funct. Anal. Appl.* **50** 233–236
- [26] Buslaev V 1998 Imaginary parts of Stark–Wannier resonances *J. Math. Phys.* **39** 2520
- [27] Sacchetti A 2014 Existence of the Stark–Wannier quantum resonances *J. Math. Phys.* **55** 122104
- [28] Buslaev V S and Dmitrieva L A 1990 A Bloch electron in an external field *Leningrad Math. J.* **1** 287–320
- [29] Simon B and Herbst I 1978 Stark effect revisited *Phys. Rev. Lett.* **41** 67-69
- [30] Longhi S 2009 Bloch oscillations in complex crystals with \mathcal{PT} -symmetry *Phys. Rev. Lett.* **103** 123601
- [31] Wimmer M, Miri M-A, Christodoulides D and Peschel U 2015 Observation of Bloch oscillations in complex \mathcal{PT} -symmetric photonic lattices *Sci. Rep.* **5** 17760

- [32] Xu Y-L, Fegadolli W S, Gan L, Lu M-H, Liu X-P, Li Z-Y, Scherer A and Chen Y-F 2016 Experimental realization of Bloch oscillations in a parity-time synthetic silicon photonic lattice *Nat. Comm.* **7** 11319
- [33] Ahmed Z 2009 Zero width resonance (spectral singularity) in a complex PT -symmetric potential *J. Phys. A: Math. Theor.* **42** 472005
- [34] Naimark M A 1954 Investigation of the spectrum and the expansion in eigenfunctions of a non-selfadjoint operator of the second order on a semi-axis *Tr. Mosk. Mat. Obs.* **3** 181–270
- [35] Schwartz J 1960 Some non-selfadjoint operators *Comm. Pure Appl. Math.* **13**, 609
- [36] Mostafazadeh A and Mehri-Dehnavi H 2009 Spectral singularities, biorthonormal systems and a two-parameter family of complex point interactions *J. Phys. A: Math. Theor.* **42** 125303
- [37] Mostafazadeh A 2015 *Physics of spectral singularities*, Trends in Mathematics 145 (Springer International Publishing, Switzerland)
- [38] Chong Y D, Ge L and Stone A D 2011 PT -symmetry breaking and laser-absorber modes in optical scattering systems *Phys. Rev. Lett.* **106** 093902
- [39] Rosanov N N 2017 Antilaser: resonance absorption mode or coherent perfect absorption? *Physics – Uspekhi* **60** 818
- [40] Chong Y D, Ge L, Cao H and Stone A D 2010 Coherent perfect absorbers: Time-reversed lasers *Phys. Rev. Lett.* **105** 053901
- [41] Wan W, Chong Y, Ge L, Noh H, Stone A D and Cao H 2011 Time-reversed lasing and interferometric control of absorption *Science* **331** 889–892
- [42] Baranov D G, Krasnok A, Shegai T, Alú A and Chong Y D 2017 Coherent perfect absorbers: linear control of light with light *Nat. Rev. Mater.* **2** 17064
- [43] Garmon S, Gianfreda M and Hatano N 2015 Bound states, scattering states, and resonant states in PT -symmetric open quantum systems *Phys. Rev. A* **92** 022125
- [44] Yang J 2017 Classes of non-parity-time-symmetric optical potentials with exceptional-point-free phase transitions *Opt. Lett.* **42** 4067
- [45] Konotop V V and Zezyulin D A 2017 Phase transition through the splitting of self-dual spectral singularity in optical potentials *Opt. Lett.* **42** 5206; corrections: 2019 *Opt. Lett.* **44** 1051
- [46] Ahmed Z, Kumar S and Gosh D 2018 Three types of discrete energy eigenvalues in complex PT -symmetric scattering potentials *Phys. Rev. A* **98** 042101
- [47] Konotop V V and Zezyulin D A 2019 Spectral singularities of odd- PT -symmetric potentials *Phys. Rev. A* **99** 013823
- [48] Borisov D and Dmitriev D 2017 On the spectral stability of kinks in 2D Klein-Gordon model with parity-time-symmetric perturbation *Stud. Appl. Math.* **138** 317–342
- [49] Kato T 1966 *Perturbation theory for linear operators* (Springer-Verlag, Berlin)
- [50] Heiss W D 2011 The physics of exceptional points *J. Phys. A: Math. Theor.* **45** 444016
- [51] Ahmed Z 2014 Handedness of complex PT -symmetric potential barriers *Phys. Lett. A* **324** 152158
- [52] Cartarius H and Wunner G 2012 Model of a PT -symmetric Bose–Einstein condensate in a δ -function double-well potential *Phys. Rev. A* **86** 013612

- [53] Zezyulin D A and Konotop V V 2016 Nonlinear currents in a ring-shaped waveguide with balanced gain and dissipation *Phys. Rev. A* **94** 043853
- [54] Levin B Ya 1996 *Lectures on entire functions*. Amer. Math. Soc. (Providence, RI)